LOW TEMPERATURE SINTERING OF SILICON CARBIDE THROUGH A LIQUID POLYMER PRECURSOR

by

Ryan Read

BS, University of Pittsburgh, 2012

Submitted to the Graduate Faculty of

Swanson School of Engineering in partial fulfillment

of the requirements for the degree of

Master of Science

University of Pittsburgh

2014

UNIVERSITY OF PITTSBURGH

SWANSON SCHOOL OF ENGINEERING

This thesis was presented

by

Ryan Read

It was defended on

March 27th, 2014

and approved by

John Barnard, Ph.D., Professor

Department of Mechanical and Material Science Engineering

Ian Nettleship, Ph.D., Associate Professor

Department of Mechanical and Material Science Engineering

Thesis Advisor: Jung-Kun Lee, Ph.D., Associate Professor,

Department of Mechanical and Material Science Engineering

LOW TEMPERATURE SINTERING OF SILICON CARBIDE THROUGH A LIQUID POLYMER PRECURSOR

Ryan Read, M.S.

University of Pittsburgh, 2014

There exists a need for a more developed and advanced cladding material for operational nuclear reactors. The current cladding, a Zirconium-alloy, is quickly approaching the pinnacle of its ability to handle the increasing fuel load demands. Also, as evidenced by the incident at Fukushima, it reacted violently with water steam at high temperatures, which created hydrogen gas and lead to subsequent explosions. Therefore, the material leading the investigation to replace the alloy is silicon carbide. Silicon carbide has been processed and manufactured through several techniques; however, this study focuses on the development of silicon carbide through the use of the polymer infiltration and pyrolysis (PIP) technique. This technique utilizes a polymer precursor, AHPCS, in accordance with low temperature sintering to enhance the density of silicon carbide. This procedure is environmentally friendly and makes use of low temperature and pressure processing parameters. The density achieved through this study was found to be 95 percent of fully dense silicon carbide. In an effort to enhance sintering and further increase density, nickel nanoparticles were added to the polymer precursor in two different proportions, 5 and 10 weight percent. The obtained densities were 96 and 97 percent, respectively. Hardness values were also obtained for the pure silicon carbide sample, 5 and 10 weight percent nickel samples. They were 2600, 2700 and 2730 HV, respectively. In addition to the recorded densities and hardness values, scanning electron and optical microscopy images were also utilized to

properly characterize the samples. From the images obtained through these instruments, it is seen that the samples appear quite dense with minimal open pores. Lastly, x-ray diffraction patterns were recorded to appropriately characterize the phase of each sample and assess any additional product formation with the addition of the nickel nanoparticles. It is apparent that the pure silicon carbide samples are crystalline in phase from the XRD examination. As for the nickel added samples, there appears to be a formation of nickel carbide. The obtained results are a promising outlook on the advancement of silicon carbide as a potential cladding material for operational nuclear reactors.

TABLE OF CONTENTS

LIST OF TABLES

LIST OF FIGURES

PREFACE

I would like to thank my adviser, Jung-Kun Lee as well as the late John Metzger. Without their initial support to enter the Mechanical and Material Science department, I would not have had the opportunities I experienced. Dr. Lee was instrumental in advancing my knowledge and understanding as a material science engineer. His dedication, support and knowledge have propelled my abilities in preparing this document. I would also like to thank my committee members, Dr. John Barnard and Dr. Ian Nettleship for their knowledge and recommendations during my time as a graduate student. I have been surrounded by a truly exceptional educational faculty. I cannot thank them enough for all they have provided me with.

I would also like to thank my research group for their levity in times of angst. They always seemed to know how to pick the spirits up when they were low. I would also like to thank them for all the time they put in to assist me in my experiments and characterizations. They provided their technical support on many of the machines that were utilized in characterizing the results for this thesis. Their experience and knowledge is greatly appreciated.

Lastly, and most importantly, I want to thank my family and friends for all of the support they have shown me and the encouragement they have provided during these years. Without them I would not be where I am today. I cannot thank my dad and mom enough for all the advice, love and support they have provided me with. It means everything to me. My grandparents have

always supplied m with continual love and support and I appreciate everything they have done for me. Lastly, I would like to thank Alana and Lass, both of them have provided countless memories and were amazing at relieving any stress or anxity I may have had.

1.0 OBJECTIVE

The objective of this research effort is to investigate and further understand the practicability of a novel processing technique for the fabrication of silicon carbide (SiC). In hopes that silicon carbide would ultimately be utilized for applications in the nuclear industry, specifically as the cladding component in retrofits of Generation III (Gen III) Light Water Reactors (LWRs) and potentially in Generation IV (Gen IV) reactors and Small Modular Reactors (SMRs).

Current reactor technology in nuclear power plants across the United States, and most of the world, resides in the use of Gen III LWRs. Research and construction of the Gen IV LWRs is currently underway; however, in comparison, the Gen III's dominate a vast majority of current reactors that have been and will continue to be in operation for quite some time, given the proper approvals from the governing authorities. Therefore, it is reasonable to believe that as long as nuclear power is still a factor in the energy production in the United States and the rest of the world, the Gen III's will likely dominate the industry for the years to come. With this majority comes a more defined understanding on the performance of these reactors under steady state as well as transient conditions. With this knowledge, it is reasonable to believe that retrofits will be performed on the Gen III's, if applicable, prior to new nuclear power plants being constructed due to economical means as well as a lack of a clear direction for nuclear waste management. Therein lays the importance of understanding and researching silicon carbide at this current moment as a cladding material for nuclear reactors as retro modifications will begin to

commence in the years to come. Researching the performance of silicon carbide now will allow for a more efficient transition from the current zirconium alloy to silicon carbide.

In the desire to further increase the ^{235}U enrichment for an extended burn-up, or additional alterations that can directly lead to a higher fissile content of the fuel; newer materials that are highly resistant to irradiation damage and corrosion may ultimately become an absolute necessity. With these requirements, it is crucial to obtain a greater understanding of what materials will ultimately succeed the current cladding in order to confirm the validity and safety of the new material. Therefore, it is important to comprehend what is currently being used and what aspects need to be improved to provide better reliability and improved safety standards.

The incident in Japan is a good example to understand what is currently being used for cladding and what potential downfalls this material possesses. A quick synopsis of the incident in Japan; the emergency generators were submerged by the tsunami that was a result of an earthquake; however, what may have been more damaging to the facility and ultimately in releasing radiation to the environment was the subsequent explosions that were a result of the hydrogen gas built up in some of the reactors. This hydrogen build up was likely due to hot steam coming in contact with the cladding material, Zircaloy-4. As the temperature increases and water comes in contact with this cladding material, hydrogen is produced, which is a hazard in any loss of coolant accident (LOCA). When comparing the use of silicon carbide as the replacement for zirconium alloys as the cladding material in nuclear reactors, it is known that silicon carbide reacts slower with water due to its chemical inertness and thus can remain in the core longer. Even with the LOCA accident, it is believed that the reaction between the hot steam and silicon carbide will not result in a build-up of hydrogen gas and consequential explosions.

For this investigation, the primary focus is on crystalline silicon carbide, which has the additional excellent properties of high strength, high modulus, excellent creep resistance, low coefficient of thermal expansion, and high-temperature stability [1-8]. Furthermore, it does not undergo phase transitions that would cause discontinuities in thermal expansion [5, 7, 9, 10]. Previously, there has been put forth a substantial effort in understanding silicon carbide based composites for various applications relating to advanced energy systems, other than for the sole purpose of nuclear technology. These advanced energy systems include but are not limited to power silicon carbide metal-oxide-semiconductor-field-transistors (MOSFETs), flue gas monitoring of gases such as carbon monoxide, nitric oxide or oxygen to help increase combustion in the boiler of coal fired power plants. In another nuclear application, SiC has been employed in radiation detectors to assist in radiation readings in specified regions in a power plant [5, 11, 12]. Ultimately, it is the goal to understand the sintering behavior with the polymer precursor as well as with the addition of nickel nanoparticles. Through this understanding a more advanced knowledge on the processing techniques of silicon carbide can be achieved.

2.0 BACKGROUND AND LITERATURE REVIEW

Silicon carbide is recognized as one of the most commonly used ceramics due to its excellent mechanical and microstructural properties in addition the properties of silicon carbide make it suitable for applications that involve high temperature, high frequency and high power [1, 2, 5, 7, 8, 11, 13, 14]. As of recently, silicon carbide is becoming known in the nuclear industry for the application that directly involves the reactor core. For instance, silicon carbide has demonstrated very low oxidation rates up to 1700 degrees Celsius and has a high sublimation temperature of 2700 degrees Celsius [13].

The application for silicon carbide is for the fuel cladding in the reactor core, which is one of three barriers of defense for the reactor. The current fuel cladding material in nuclear reactors is zirconium-based alloys. This type of cladding has raised concern in regards to safety as seen by the Fukushima Dia-Ichi accident as previously discussed. To help further mitigate these types of accidents, silicon carbide has been introduced as a leading candidate to replace the zirconium-based alloys for the fuel claddings in current and future designs of reactor cores. Cladding materials that degrade at a slower rate in severe accidents is also an important feature that is crucial to sustainability and performance. Therefore, it is likely that replacing the current zirconium-alloy based fuel cladding will be a retro-modification on Gen III reactors in the future.

It is believed that silicon carbide will not result in a hydrogen explosion if reacted with water and steam due its chemical inertness. This is one of the greater potentials of silicon carbide

as opposed to the current zirconium-based alloys currently used in operating reactors around the world. In a comparison performed by Kwangwon Ahn, of Massachusetts Institute of Technology, where silicon carbide was compared to Zircaloy-4 during a large break loss of coolant accident (LBLOCA), it was shown that the silicon carbide has a higher safety margin than the Zircaloy-4 cladding [3]. This is partly due to the fact that silicon carbide has higher yield and ultimate strengths as opposed to the Zircaloy. In another analysis of a similar accident scenario, it was shown that zirconium alloys corrode at an elevated pace in steam at the elevated temperatures seen in a LOCA [2]. A material with a high melting point and chemical inertness would be most desirable for this situation. These are just two examples of studies performed where it can be seen that a new cladding material is required to replace the current material of zirconium based alloys.

2.1.1 Current Cladding Material, Zirconium Based-Alloys

To briefly touch upon the current cladding material, zirconium based alloys; the following paragraphs will outline some key aspects of the current material as well as touch upon some elements that are undesirable. Zirconium based alloys allow for a high melting point, as well as high mechanical strengths. They also allow for high corrosion resistance and a low neutron absorption cross section for thermal neutrons [6, 15]. This low cross-section is important for the economics of the reactor and ensuring that criticality does not become a major concern during operation of the nuclear reactor. Currently, the cladding materials possess approximately 97-99% zirconium with small constituents added to optimized properties [2]. These constituents consist of tin, iron, chromium, niobium and nickel, which can lead to secondary phase particles due to the solubility of these constituents in zirconium. The chemical compositions as well as the

size distribution and number density of these secondary phase particles play a critical role in the reactor performance of a cladding alloy. For example, they have an effect on the creep, growth, corrosion and hydrogen pickup [2].

Enriching the uranium dioxide fuel is required for LWR's and that enrichment is typically between 3 and 5 %. Therefore, it is necessary that the cladding material be able to support the burnup of this fuel, which can reach a peak value of around 75 MWd/kg U [16]. The longevity and lifetime of the zirconium cladding is based upon the corrosion properties it exhibits, for example, the association with absorbed hydrogen. With increasing hydrogen concentrations above the solid limit for zirconium, hydride precipitates form, which have a negative effect on the performance of mechanical strength and reduces the ductility of the cladding [2]. The chemical equation for the oxidation reaction of zirconium can be seen in Equation 1. The mechanism by which corrosion occurs in the zirconium based alloys is by the diffusion of oxygen ions through gaps from the water/oxide interface to the oxide/metal interface [15]. This process is impeded when there is a break in oxide layer as it becomes thicker. Thus, the diffusion of oxygen ions in the oxide layer controls the time it takes to break the oxide layer.

$$\mathbf{Zr + 2\ H_2O \rightarrow ZrO_2 + 2\ H_2}$$

Equation 1 - Oxidation Reaction of Zirconium

If nitrogen is present in the metal, it can take up atom positions that normally would have been filled by oxygen in the crystalline oxide net and leads to an increased number of gaps, which then causes a larger diffusion of oxygen. If tin is present in the metal, it is incorporated in the crystalline oxide net, in zirconium atom positions. If both tin and nitrogen are present in the metal, they tend to associate which decreases the number of gaps and in turn decreases the diffusion of ions of oxygen [15]. The mechanical properties of the zirconium alloy tubes for

cladding depend largely on the crystallographic texture obtained during the configuration process.

A factor that can be affected by the yield and strength of the zirconium alloy cladding is creep, which is a deformation under the action of a stress that is normally below the yield strength and is dependent on time and temperature [15]. Fuel rod performance can be greatly affected by the inward creep of cladding early in core life and outward creep later in life. In many countries, a limiting burnup, fuel design, and safety criterion require the fuel clad outward creep rate to be no larger than the fuel pellet swelling rate [17]. This requirement accounts for the situation in which the rod internal pressure exceeds the primary system pressure, possibly due to a large release of fission gas, and induces outward cladding creep. If the rate of cladding creep exceeds the rate of pellet swelling, the pellet-clad gap will re-open [17]. This can be seen in Figure 1. It is believed that silicon carbide will not present this issue of creep that would result in the pellet-clad interaction.

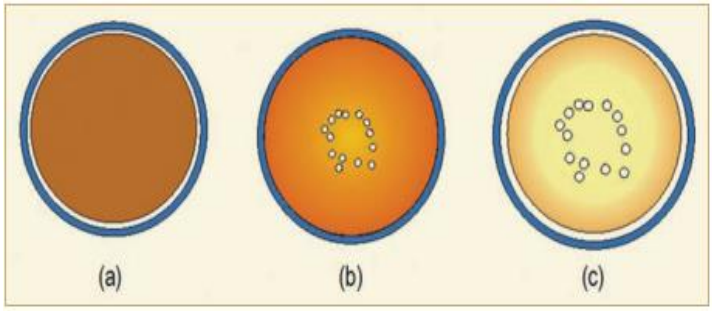

Figure 1 - (a) Low burnup with noticeable pellet-cladding gap, (b) Medium burnup with no pellet-cladding gap and (c) High burnup in high power rod with significant fission gas release with reopening of pellet-cladding gap [17].

Corrosion is not the only factor influencing the lifetime of the zirconium cladding; irradiation also plays a key role in determining the performance the cladding material. Irradiation has been seen to lead to alterations in the microstructure of a material, for instance, buildup of

dislocation loops and dissolution of the secondary phase particles as previously mentioned. These changes play a major reactor on the in-core reactor performance during operation. As with most materials in industry today, it is thought to push them as far as they can go to get a better understanding during certain situations; however, for the case of the zirconium alloys as cladding material, they may be quickly approaching their limits for increased fuel enrichments and burnups. Therefore, it is believed that a newer, more advanced material will be required to handle these fuel duties in current reactors as well as future reactors.

As previously mentioned, silicon carbide is the leading candidate for this application. Silicon carbide provides great sustainability for future alterations and also allows for a larger safety margin to be achieved. The mechanical, thermal and intrinsic properties of silicon carbide propel it forward to be further studied and analyzed for application as the fuel cladding. Silicon carbide does have an abundance of positive attributes; however, it does face its challenges as well. The main challenge that is apparent is the joining of silicon carbide at the end caps of the cladding material to enclose the fuel [18, 19]. This challenge is quite arduous as silicon carbide does not directly bond easily with silicon carbide. Also, it cannot be simply welded as the case with the zirconium cladding. EWI have devised a joining approach that makes use of an Al-Si alloy to successfully join the ends of the fuel cladding [19]. The actual joining of silicon carbide is not essential to this study and is out of the purview of the researching scope of the project. It is important to recognize that this is a challenge that must be faced once a desirable manufacturing method of silicon carbide has been established.

In a study performed by Ceramic Tubular Products in regards to silicon carbide as fuel cladding as an alternative to the zirconium alloy, they had found that silicon carbide performs well during accident scenarios as well as with high burn-ups and power densities. For the

accident scenarios, it was seen that silicon carbide will not balloon out in shape during design basis and beyond design basis accidents, thus not blocking critical flow paths for cooling of components. Silicon carbides ability to perform at high temperatures will likely survive the departure from nucleate boiling (DNB) accidents in LWR's and similar dryout accidents in boiling water reactors (BWR's). In order to take advantage of this feature, it is suggested that the cladding be coupled with an advanced fuel form in order to prevent excessive fuel temperatures [20].

2.2 METHODS OF MANUFACTURING SILICON CARBIDE

In order to better understand the potentials of silicon carbide it is necessary to retrace the processing techniques of silicon carbide through the years. The three major techniques that will be discussed include; the Acheson Method, Chemical Vapor Deposition (CVD), Reaction Bonded Silicon Carbide, Use of Additives and Polymer Infiltration and Pyrolysis (PIP). Each of these techniques varying in the processing parameters; however, each one manufactures the desired product of silicon carbide. Each technique varies in processing temperature and pressure as well. These techniques will be discussed in detail in the following paragraphs.

2.2.1 The Acheson Method

The Acheson Method was named after its inventor, Edward Goodrich Acheson in 1890. This process consists of heating silica sand and powdered coke to high temperatures in an iron bowl.

Figure 2 displays a cross-section of an Acheson furnace to which silicon carbide is manufactured.

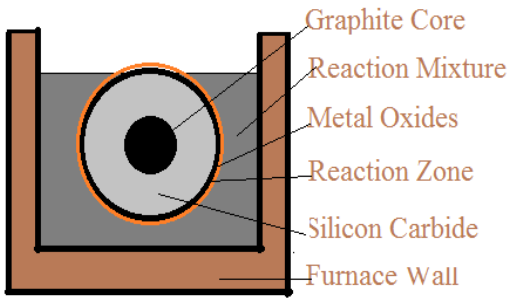

Figure 2 - Cross-Section of Acheson Furnace

In the Acheson graphite electric resistance furnace, an electric current is passed through the graphite core. The electric current heats the graphite and other materials to a temperature greater than 2500 degrees Celsius, allowing them to react, producing a layer of silicon carbide around the graphite core. During this process, carbon monoxide (CO) is given off as seen by the following reactions. These four chemical reactions describe in detail the process that produces silicon carbide [21]:

1. $C + SiO_2 \rightarrow SiO + CO$
2. $SiO_2 + CO \rightarrow SiO + CO_2$
3. $C + CO_2 \rightarrow 2CO$
4. $2C + SiO \rightarrow SiC + CO$

Equation 2 - Silicon Carbide via Acheson Process

The crystalline silicon carbide that is obtained via the Acheson method has been seen to occur in varying polytypes as well as purity [12]. In addition, while the heating process is proceeding, with varying differences in the distance from the graphite resistor heat source of the

Acheson furnace, different colored products could be formed [12]. The product that is manufactured will likely have large grain sizes and customarily tainted with oxygen. Common impurities, such as nitrogen and aluminum are found which can have adverse effects on the electrical conductivity of silicon carbide. Thus, the trademark name carborundum, is satisfactory for usage in the applications of abrasive and cutting tools [12].

2.2.2 Chemical Vapor Deposition (CVD)

The technique of chemical vapor deposition is easily recognized as one of the more familiar methods to producing and synthesizing highly crystalline beta-silicon carbide [14]. This process can produce solid silicon carbide from a gas phase reaction of relatively low temperature, approximately 1173 to 1373 Kelvin without the use of sintering aids. However, these techniques possess the largest variability in terms of deposition parameters. For example, these chemical reactions can include thermolysis, hydrolysis, reduction, oxidation, nitration as well as carboration [12]. This is dependent on what precursor species are used in the reactions. Control over the processing temperature is critical for CVD as this regulates the process thermodynamics and kinetics [1]. This technique involves deposition of a solid material on to heated or activated surface by the reaction of a gaseous phase [22]. Common reactant gases include methyltrichlorosilane (CH_3SiCl_3), or ethyltrichlorosilane ($C_2H_5SiCl_3$) in combination with hydrogen as the carrier gas [14]. Both reactions are seen in the following equations, respectively.

$$CH_3SiCl_3 \rightarrow SiC + 3HCl$$

Equation 3 - Methyltrichlorosilane Gas Reaction to Form Silicon Carbide

$$C_2H_5SiCl_3 + H_2 \rightarrow SiC + 3HCl + CH_4$$

Equation 4 - Ethyltrichlorosilane Gas Reaction to Form Silicon Carbide

Methane, CH_4, seen in Equation 5 can be easily decomposed to free carbon with a generation of hydrogen as seen by the following equation. The free carbon that is produced has the potential to lead to undesirable carbon layers or carbon-rich phases [14].

$$CH_4 \rightarrow C + 2H_2$$

Equation 5 - Decomposition of Methane to Free Carbon

Another common reaction to produce SiC in its various shapes and forms such as powders, whiskers as well as nanorods can be seen in the following equation. Amorphous fine silicon carbide powders have been prepared by CVD method in the SiH_4-C_2H_2 system under nitrogen as a carrying gas [12].

$$2\,SiH_4 + C_2H_2 \rightarrow 2SiC + 5H_2$$

Equation 6 - Silicon Carbide Formation by way of Silane

The methods by which silicon carbide is produced by way of the chemical vapor deposition technique are inherently toxic, as these gases need special ventilation and precautions to avoid any harmful exposure. Although this method is quite simple in terms of what needs to be done, it does leave a lot of room for variation and error in a desirable end product. Also, since these gases are not overly common and require special precautions, this technique can be rather expensive as well as unfavorable for the environment. Challenges in CVD include gas phase nucleation and homogenous reaction occurring due to supersaturation of the reactive species in the gaseous phase. Also control of microstructure and residual stresses is a matter of concern in CVD process [1]. Alternative methods to this technique are hard to come by as often they do not yield such high stoichiometric results; however, one method that may be able to directly compete with the chemical vapor deposition method is the polymer infiltration and pyrolysis technique.

2.2.3 Reaction Bonded and Sintered Silicon Carbide

Two different techniques in forming silicon carbide include reaction bonding and sintering. Both methods of silicon carbide possess high temperature strength and wear resistance, as well as good thermal shock resistance among other mechanical properties.

Reaction bonded silicon carbide is manufactured through infiltration of molten silicon into mixtures of porous silicon carbide and carbon. Through this process silicon reacts with the carbon forming more silicon carbide, which bonds the initial silicon carbide particles. Ultimately, there is residual silicon present as it does not completely react with all the carbon to form silicon carbide. Therefore, the final constituents present include the original silicon carbide, the reaction formed silicon carbide and as mentioned the residual silicon. The final silicon carbide to silicon ratio can be controlled by the original silicon carbide to carbon ratio. As seen in Figure 3 is a schematic of process that produces the reaction bonded silicon carbide. This process allows for large and complex shapes to be created due to low process shrinkage (< 1%), the reaction bonding process fills the void space via infiltration, shrinkage is more prevalent in sintering.

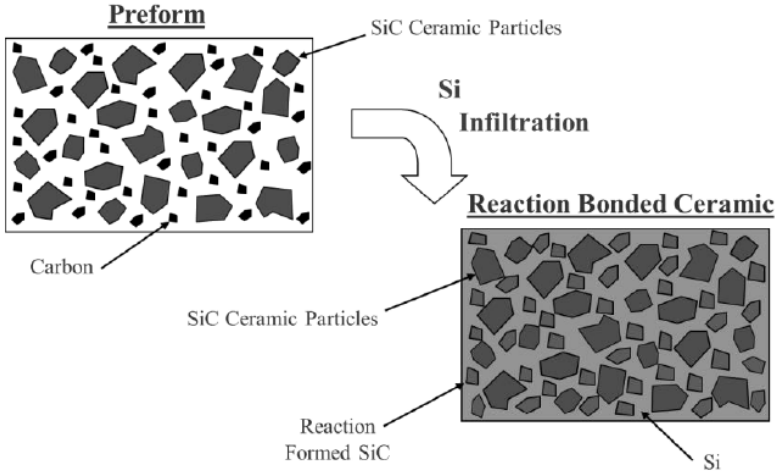

Figure 3 - Process Schematic of Reaction Bonded Silicon Carbide [23]

The other method to manufacture silicon carbide is through sintering. This material is produced from pure silicon carbide powder with non-oxide sintering aids. The powder is compacted by forming processes such as die or isostatic pressing as well as injection molding. Once the powder is formed and compacted it is then sintered in an inert atmosphere at temperatures above 2000 °C. From here, the resulting sintered silicon carbide can be machine to desired tolerances. Sintered silicon carbide has many applications such as armor, bearings, mechanical seals as well as heat exchanger tubes.

2.2.4 Additives to Enhance Densification

Additives were utilized in the 1970's to enhance the densification of silicon carbide. Initially, the simultaneous additions of boron and carbon allowed for solid state sintering and ultimately greater densification. Through the addition of these additives a high density was achieved at temperatures above 2000 °C. This occurred through the reduction of the superficial energy of the grains, due to the boron, and the reaction with the residual silica with carbon [24]. These additives greatly improved the shrinkage kinetics of silicon carbide [25]. A study was conducted on the properties of silicon carbide – boron carbide that was obtained by way of a pressureless sintering process. A focal point of the investigation was to improve mechanical properties that would be useful for applications in the energy sector. Ultimately, this pressureless sintering process that contained boron carbide as a secondary phase increased the sintering rate and reached a higher density at 2150 °C when compared to the solid state mechanism in the sintering of silicon carbide.

Other additives such as alumina oxide as well as ytrria oxide were utilized in the attempts to enhance the sintering rate as well as possess the capability to control the grain growth. The

pathway through the use of these additives is generally attributed to liquid phase sintering. The addition of the metal oxides results in a liquid phase formation at elevated temperatures. During the sintering process, this formation behaves in congruence with mass transport [26, 27]. This technique allows for lower processing temperatures in the realm of 1800 to 2000 °C as compared to solid state sintering where the temperatures were above 2100 °C. In addition to the lower processing temperatures, the use of these rare earth oxides allows for pressureless sintering of the silicon carbide. However, a major issue with the use of these additives to enhance the sintering behavior of the silicon carbide is the potential reaction of silicon carbide with the oxides. The weight loss experienced during these reactions can be attributed to the formation of gaseous byproducts [28]. As seen through previous studies, the sintering conditions impact the composition of the gaseous byproducts, which is ultimately the mass lost during the reaction [27, 28]. In order to prevent a large amount of mass lost during the reaction due to the formation of gases; it has been common practice to make use of a powder bed, consisting of a mixture of silicon carbide and alumina oxide. Ultimately, through processing variations, this technique has resulted in a highly dense silicon carbide material that possesses good mechanical properties.

2.2.5 Polymer Infiltration and Pyrolysis

As seen by the previous examples of manufacturing silicon carbide, their processes were based around shaping fine ceramic powders. Through sintering phases, shrinkage occurs, typically in the range of 15% which ultimately limits the geometrical accuracy. To improve the precision and intricacy, machining must accompany the process to reach a desired end product. In addition to machining, high temperatures are also required and a downside of the required high temperatures

is the use of extra energy [13]. Therefore, an alternative technique must be utilized to avoid the downfalls of the previous processing routes.

The polymer infiltration and pyrolysis technique is a method to fabricate ceramic matrix composites (CMC's), which is a non-powder based process. In this method, a low-viscosity polymer is vacuum infiltrated into the reinforcing structure, which is then followed by pyrolysis. A low viscosity polymer that is often used is allylhydridopolycarbosilane (AHPCS), although there are several other polymer precursors that can be used. This specific polymer precursor will be discussed more in detail in the following section. The atmosphere inside the heating chamber during the pyrolysis stage is often an inert gas, such as argon, which is designed to prevent any oxidation of the silicon carbide as well as condense organometallic compounds into inorganic materials [1]. This process is much simpler than the procedure for CVD and also is more environmentally friendly as no toxic gases are required to complete the reaction.

Figure 4 shows possible decomposition pathways of the polymer precursor. The top diagram is representative of when the space between silicon carbide particles was only partially filled the polymer precursor and consequentially, sintering would result in larger pores. The lower of diagram displays when the space was completely filled with the polymer precursor, thus resulting in smaller pores after sintering [29].

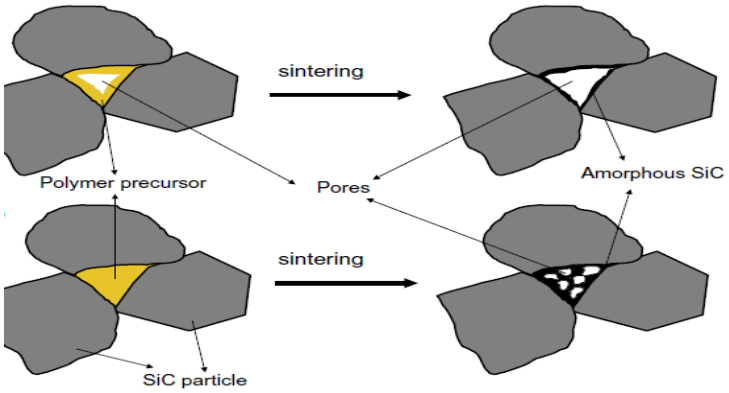

Figure 4 - Diagrams of Decomposition Mechanisms from Polymer Precursor [29]

This method is rather new when compared to the previous methods; however it does have some advantages to manufacture silicon carbide via this procedure. The fibers are relatively unharmed and damage is prevented due to the low processing temperature that is required for pyrolysis. There is good control of the microstructure as well as matrix composition. Reinforcing phases may be introduced as either fibers or particulates. This process also offers near net shape fabrication. Another advantage is that no residual silicon present in the matrix. Lastly, fabrication requires almost no pressure. However, to these advantages come some disadvantages. These can include; long fabrication time is needed to achieve high density samples, as multiple infiltration-pyrolysis cycles are required to reach this state, as well as there is often residual porosity in the samples that can reduce the mechanical properties of the composite.

2.3 LIQUID PHASE SINTERING

Liquid phase sintering (LPS) was found to occur during the addition of rare earth oxides to silicon carbide in hopes of enhancing the sintering behavior. As previously mentioned, the temperatures typically seen during this process are between 1800 and 2000 °C. Interest in liquid phase sintering was increased in the late 1990's due the fact that the materials possessed superior mechanical properties when compared to solid state sintering. It has been seen that the powder characteristics have an impact on the sintering of silicon carbide. For example, free carbon is detrimental in liquid phase sintering due to its tendency to react with the oxide additives and eventually release the gaseous byproducts that were produced during the sintering [25]. The presence of SiO_2 promotes the formation of liquid and enhances the densification of silicon carbide.

In liquid phase sintering of silicon carbide, alpha-silicon carbide is more commonly used as opposed to beta-silicon carbide. This is mostly due to the fact that the alpha form has greater stability at higher temperatures. In addition to the elevated temperature stability, it has been seen to result in fine, equiaxed microstructures [25]. However, if fracture toughness was a primary concern, the use of beta-silicon carbide would be desired as the starting powder. This is due to the beta to alpha transformation at about 1950 °C results in coarse, elongated microstructures. These elongated microstructures have been shown to increase the fracture toughness of silicon carbide by either crack bridging or deflection [25, 30]. Previous studies have shown that the phase transformation from beta to alpha does not directly enhance the densification of silicon carbide. To that extent, the beta-silicon carbide has been shown to possess less densification due to the elongated grains as opposed to alpha-silicon carbide.

As with any processing technique there are often factors that have pronounced effects on the outcome. In liquid phase sintering of silicon carbide the most important factors include but are not limited to: characteristics of the starting powder; sintering method and corresponding parameters such as time, temperature and pressure; sintering atmosphere, whether it is under vacuum or under an argon or nitrogen ambience; amount and composition of the liquid phase as well as processing prior to sintering [26, 27]. The characteristics of the starting powder are that of the grain size distribution as well as oxygen and carbon content. Major requirements on the liquid phase sintering medium include: sufficient volume fraction of liquid exhibiting complete wetting of the solid phase as well as contain solubility of the solid in the liquid [26, 27]. The transport properties of the liquid phase are dependent on the chemistry as well as volume fraction, where these factors are influenced by the densification parameters as well as the additives utilized. Fabrication procedures ultimately control the densification behavior as well as

the grain growth during liquid phase sintering. The increase in strength, when compared to the solid state processing technique, can be attributed to the reduced grain growth obtained through liquid phase sintering. In the long run, the mechanical and chemical properties of the liquid phase sintered silicon carbide will be affected by the intergranular microstructure, which can be either glassy or possess some partial crystalline phase, where at high temperatures the glass will soften and have a decrease in these properties [26, 27].

2.4 USE OF AHPCS IN MANUFACTURING SILICON CARBIDE

As previously mentioned, the polymer precursor that is often used in the manufacturing of silicon carbide by way of the polymer infiltration and pyrolysis technique is allylhydridopolycarbosilane (AHPCS). Typically, AHPCS can be purchased for commercial purposes from Starfire Systems Inc., who is located in Malta, New York. AHPCS is a very high purity polymer precursor that yields a stoichiometric ratio of 1:1 upon complete pyrolysis of silicon to carbon, with hydrogen as a remainder. In addition to this favorable stoichiometric ratio, it has relatively low shrinkage after going through the pyrolysis phase. It is stated by Starfire Systems that trace contaminating elements are present at the ppm level.

The structure of the AHPCS can be seen in Figure 5. AHPCS has been studied and researched as a binder for ceramic powders and matrix source for ceramics composites that were derived from polymer precursors. In addition, it has also been utilized in the production coatings based from silicon carbide as well as joining composite and monolithic ceramic components [22]. Some relevant properties of AHPCS can be seen in Table 1. Through heating the polymer precursor, a dry and partially cross-linked solid is formed at approximately 300 ◦C [13]. Through

further heating of the polymer sample, more cross-linkage is formed in addition to the loss of low weight oligomers and hydrogen gas until alpha-silicon carbide is formed at near 900 ◦C [13]. According to the manufactures specifications, a fully ceramic, amorphous silicon carbide is formed between 850 and 1200 ◦C with minimal shrinkage [13]. Slow heating is favored in this application of AHPCS, as the slower heating rate can result in a better yield. The slow heating rate is approximated to be about 1 ◦C per minute until the temperature reaches about 650 ◦C. This slow heating favors the lower temperature curing of the polymer precursor that is involved in the competitive process of gas evolution by decomposition of the lighter molecules releasing H_2 and polymerization. This stage is crucial for filling the porosity [13].

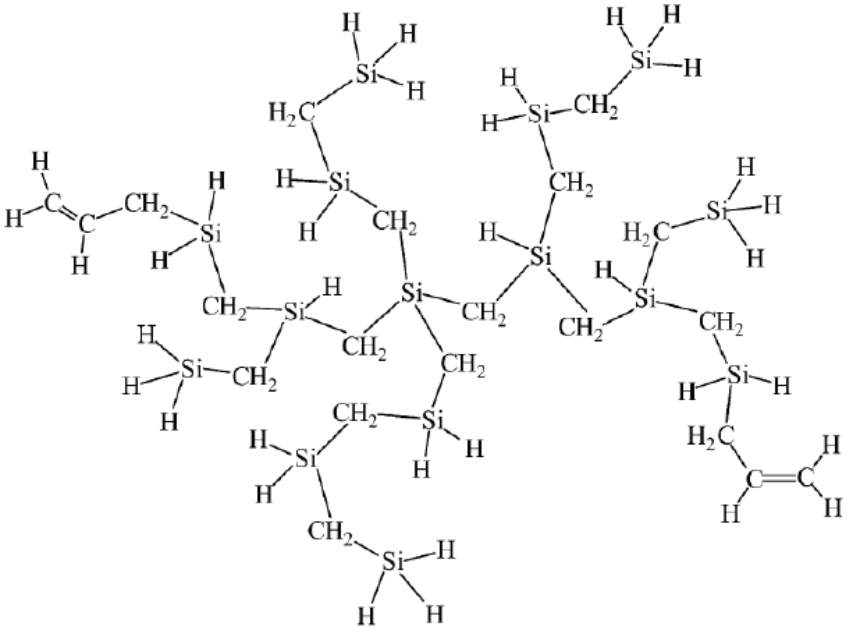

Figure 5 - Chemical Structure of AHPCS [22]

Table 1 - AHPCS Properties

Property	**Allylhydridopolycarbosilane (**AHPCS)
Density ($\frac{g}{cm^3}$)	0.998
Viscosity (cps)	80 to 100
Flash Point (◦C)	89
Appearance	Clear, yellow-amber liquid
Solubility	Acetone, Toluene, Hexane; insoluble in water
Nominal Cure Temperature (◦C)	250 to 400
Surface Tension ($\frac{dynes}{cm^2}$)	30

There have been several studies completed on the use of AHPCS in the polymer infiltration and pyrolysis method. In these studies, density was an important parameter that was quantified to a rather distinguishable degree. In addition to the measurement of density, other parameters such as hardness, fracture toughness, effect of temperatures of pyrolysis on the performance of silicon carbide as well as optical and scanning electron microscope images. Being able to quantify the results achieved through various testing of silicon carbide samples allows for greater understanding and the ability for others in the future to make alterations to enhance the performance of the silicon carbide.

A research effort by Moraes and Interrante studied the effects of processing, fracture toughness and Vickers hardness of AHPCS-derived silicon carbide. In this study, the first pyrolysis stage was to 1000 °C followed by subsequent reinfiltration and pyrolysis steps with AHPCS. During the subsequent reinfiltration phases, the ultimate processing temperatures these samples would reach were altered. The temperatures were 1200, 1400 and 1600 °C. According to

Moraes and Interrante, this fabrication process simulated the production of the desired matrix phase for CMC's via the PIP method [31]. The first analysis they performed was the density calculation. The method they chose to calculate the density of their samples was the Archimedes Principles method. For the temperatures of 1000, 1200, 1400 and 1600 the densities were 2.3, 2.5, 2.6 and 2.9 grams per cubic centimeter, respectively. Also, they were to determine the percentage of open pores in their samples. These values were 2, 0.2, 1 and 9 volume percent, respectively. The next analysis they performed was the fracture toughness of their samples and they performed this through the use of the single edge V-notched beam method. The results of this analysis was 1.40, 1.65, 1.67 and 1.47 $MPa*m^{0.5}$, respectively. As for the Vickers hardness, the method was simply the Vickers indentation of the samples and the load was 1000 grams. These values were determined to be 12, 13, 11 and 9 GPa, respectively [31]. Through their findings, they believed that this experimentation was successful in that it effectively fabricated monolithic specimens of precursor derived ceramics for conventional mechanical property testing [31].

In another study conducted by Berbon and Calabrese into the effect of 1600 °C heat treatment on silicon carbide composites fabricated by PIP with AHPCS. In contrast to the previous study of Moraes and Interrante where 10 cycles of reinfiltration and pyrolysis were required, this study only required 6 subsequent cycles to achieve satisfactory composite density. However, this study compared the differences between polymer-derived and slurry derived composite. For their samples, they infiltrated two identical sheets of woven carbon fiber fabrics with only AHPCS polymer and the other with a slurry of AHPCS and silicon carbide powder. For the slurry-derived samples, 10 volume percent of alpha silicon carbide was mixed to the AHPCS liquid through ball milling [32]. According to their findings, the slurry derived

composite has roughly 25 percent higher strength than simply the polymer derived composite. Then the heat treatment of 1600 °C was administered to both sheets and the strength of the polymer derived composite decreased by approximately 60 percent, whereas the slurry derived composite was unchanged [32].

In another study completed by Shih *et. al,* on the effect of mixing methods and PIP cycles on the densification of silicon carbide inert matrix through a polymer precursor route studied the effects of density, pore distribution and microstructure. For this experiment, the researchers mixed coarse and fine particles of beta-silicon carbide in a ratio of 60:40, respectively [33]. In addition to the mixing of coarse and fine particles, they studied the effects of altering the atmospheric pressure that these samples would endure during the infiltration process before the samples would be pyrolyzed. The first experiment would have the atmosphere at 1 atm by way of vacuum. The pellets were infiltrated for 24 hours. As for the second experiment with altering the infiltration pressure, it was recorded that 10 MPa of ultra-high purity argon gas was used. Again, the samples were infiltrated for the same time duration of 24 hours. Shih *et. al*. concluded that there was an increase in theoretical density, approximately 4.8%, when using the 1 atm pressure after the first infiltration and pyrolysis process. When analyzing the open pores, it was noted that they had diameters smaller than 10 nanometers [33]. However, when a second infiltration and pyrolysis experiment was attempted, there was no discernable change in density or pore distribution. As for the results stemming from the ultra-high purity, high pressure argon gas, the results showed some improvement when compared to the 1 atm pressure. A higher theoretical density was achieved, by about 1%, after two successive cycles. As for the pore diameters smaller than 10 nanometers, they were still hard to infiltrate and close by the PIP even with this high pressure [33].

As it can be seen from these studies, AHPCS has been researched in various ways, ultimately attempting to better understand how to produce a more dense, better packed silicon carbide samples. Therefore, from the understanding of previous practices and experimentations, it can be ascertained that a method to produce silicon carbide by way of the PIP method through the use of a polymer precursor, AHPCS, can be designed and implemented to successfully achieve highly desirable results in terms of important parameters and properties for required applications.

2.5 FREEZE CAST

The freeze cast method is a processing technique that is often used to construct macroporous ceramics with controlled porosity [34]. Through the use of the freeze cast method, directional freezing of a liquid suspension of ceramic particles can be accomplished. Once the liquid suspension is frozen, the solid phase is sublimed, yielding a porous green body that can ultimately be sintered to densify the ceramic. There are three main processing routes to create macroporous ceramics, which include; replication, direct foaming and templating. The first two are not the target of the investigation and will no longer be discussed; however, freeze casting falls under the mode of templating. Templating is when a non-ceramic material is utilized as a template for the pore structure of the ceramic material. The template is then successfully removed by the appropriate means such as freeze drying or thermal decomposition [34].

The crystals that are created during the freezing phase are the template for the desire pore channels, which are later removed as mentioned. This method is quite simple and has good flexibility in terms of processing parameters, which are two of the major reasons as to why this

method has attracted noteworthy attention. Through the creation of porous ceramics with an open pore structure, filters and supports for catalysts and absorbents can be more applicable. In these, high permeability and large surface area is required and hence why it is crucial to maintain and control pore structure, porosity, pore size as well as distribution in these materials [35].

The underlying idea behind the freeze casting technique is to initially create a liquid dispersion of ceramic particles, which is then poured directly into a mold and solidified then followed by sublimation to remove the frozen solid. Typically, the amount of ceramic particles is in the range of 10 to 40 volume percent, although others have experimented with altering the amount of solids loading. Figure 6 is a schematic of the freezing process.

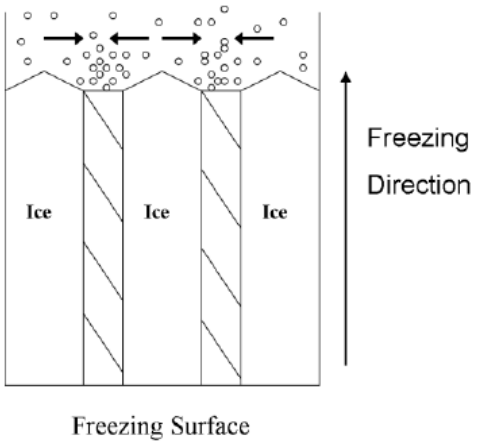

Figure 6 - Mechanism of Freeze Casting Processing [34]

The ceramics particles must be rejected from the growing crystals during the freezing process [34]. As long as the solidification phase occurs below the critical velocity, the ceramic particles will be rejected from the solid-liquid interface [34]. In this process, it is crucial that solid-liquid interface does not become planar, as if this is to occur; the ceramic particles are more likely to end up on one side of the sample. This is an undesirable result as the sample would be useless in controlling pore structure and so forth. The rejected particles will accumulate between the growing crystals and will form what will ultimately transpire to being the pore walls [34].

Once the freezing aspect is complete, the freezing-drying phase can commence as this done to prevent and avoid drying stresses that would ultimately result in cracking or warping. This is done by placing the frozen sample inside a vacuum chamber and lowering the pressure beneath the triple point of water, which will cause sublimation. Once the water has been sublimed, the sample will have unidirectional pore channels and then it can be sintered to increase density or it can undergo other processing techniques.

Through the use of the freeze cast technique, the resulting structure can be altered through varying different parameters during freezing. Some of the parameters include; solids loading, temperature during the freezing process, sintering temperature of the green bodies, using another liquid instead of water for the dispersion as well as varying the concentration of the dispersion agent used. These are just some of the more studied parameters that have been altered and examined to understand how they affect the freeze casting of ceramics. For this study, only the effects of solids loading will be examined as the freezing temperature will remain constant, as will water and the concentration of the dispersion agent used. Therefore, it is important to understand what has been previously accomplished on the effects of solids loadings in ceramics through the use of the freeze cast method.

Solid loading is known as the amount of starting ceramic particles, most commonly seen in terms of volume percent. Start ceramic particles are often alumina-based; however, for the investigation of this study it is strictly silicon carbide. The size of the starting silicon carbide particles is considered to be a relevant factor. This is due to the fact that sub-micrometer sized powders give way to large surface areas, short diffusion distances as well as a large thermodynamic driving force for densification [36]. In work completed by Ferreira and Diz, they were able to increase the green density of monomodal silicon carbide powders from

approximately 60 percent theoretical density (TD) to nearly 75 percent TD. This was dependent on the ratio of fine to coarse powders as well as the ratio between average sizes of the components in the mixture [36]. After which, a constant and moderated solids loading of 62.5 weight percent was utilized, which had resulted in partial segregation. The segregation was noticeable due to the different color of starting powders; the inner region was rich in gray, coarse particles, whereas the outer region was mostly green fine particles.

Further research efforts were conducted by both Ferreira and Diz into the most effective deflocculant for aqueous slurries as well as studying the volume and solids loading influence on the green density of the slip casted bodies. They had found that the packing density increases as the amount of dispersant added increases until a maximum is reached, after this point, the density begins to decrease. This finding is based upon a given solids loading to start with. At the lower solids loading there is more prevalence of segregation and the particles do not pack homogeneously. With the lower solids content, particles have more freedom to rearrange spontaneously during the deposition stage as they occupy the lowest free energy position at the suspension interface [36]. As the solids content increases, the suspension becomes more populated with particles and the deposition rate increases. Collisions and interference between particles limits the potential for rearranging as well as separation as found in the lower solids content samples. The ability for the sample to pack tightly is determined from these two phenomena. At high solid loadings, they discovered that the slip viscosity is high enough to thwart particle rearrangement, separation and the escape of entrapped air bubbles. These result in a lower degree of packing and thus a broader pore size distribution [36].

3.0 MOTIVATION

Energy consumption throughout the world will only continue to rise for centuries to come and for that reason it is vital that the supply meet the demand. Currently, coal fired power plants are dominating the global energy sector, as they produce a substantial amount of energy. However, as it is widely known, they are infamously recognized for their release of toxic pollution and greenhouse gases into the atmosphere. With increasingly strict regulations set forth upon these power plants to limit the amount of pollution emitted to the atmosphere, other energy sources will need to produce the power that these plants will ultimately fail to provide. These restrictions have caused several coal fired power plants to construct expensive modifications such as flue-gas desulfurization systems to restrict the release of NO_x and SO_x into the atmosphere or alternatively shut the power plant down. With the closings of coal fired power plants comes the reduction of energy suppliers to the national energy grid, thus raises the importance of nuclear power as they have minimal to near zero release of toxic and greenhouse gases.

In lieu of these environmental restrictions established by governing agencies, nuclear power has had renewed interest, as it is known at this time that alternative energy sources such as solar and wind cannot provide for what coal will ultimately fail to provide in the future. Although, with nuclear power comes concerns regarding weapons proliferation, nuclear waste management as well as reactor safety. In terms of reactor safety, there have been three major reactor accidents over the course of nuclear power plants, which include: Chernobyl, Three Mile

Island and most recently Fukushima Dai Ichi. Each of these accidents had consequential effects for human safety. Of the three, Chernobyl was arguably the worst in terms of devastation to the population and ecosystem surrounding the facility in regards to the amount of radiation released.

Through simulations and knowledge of the properties of silicon carbide, it is believed that it possesses the ability to remain in the core for an extended period of time, which would allow for extra energy to be squeezed out of the fuel rods before refueling is necessary. The rods are typically replaced approximately three to five years into operation in the reactor. A major limiting factor for the replacement of these rods is due to the degradation of the cladding. Another advantage of having the ability to leave the fuel rods in the reactor for an extended period of time would be that the amount of waste produced would decrease, on a volume basis. From this incident alone, it can be seen that the production of hydrogen gas from the reaction of zirconium and steam is an ill-effect of the current cladding material that needs to be addressed moving into the future with increased safety standards. Therefore, more advanced processing techniques of silicon carbide need to be developed that would better suit the needs nuclear reactors desire. Through this investigation a polymer infiltration method will be utilized, as will a freeze casting method that will provide a porous material with a rigid framework.

The polymer infiltration and pyrolysis (PIP) method has stimulated interest in producing high yield ceramics from polymer ceramic precursors. This technique has allowed for near net-shape fabrication of ceramic based materials for various applications [1, 31, 37, 38]. Instead of using only solid state powders, liquid-type polymer precursors of silicon carbide will be utilized together to develop silicon carbide for the purpose of cladding material. The raw, liquid-type materials of this method are element-organic polymers whose structure and composition can be customized and altered. A recent development of high-yield preceramic precursors has enabled

the fabrication of ceramic-based materials by this PIP method. Polymer derived ceramic materials offer unique advantages such as ability to fabricate net-shaped components, the incorporation of matrix reinforcements, lower processing temperatures, and perhaps most importantly, relatively easy control over the microstructure [1, 33, 37, 39]. Multiple repetitions of infiltration and low-temperature annealing steps will allow for high-density ceramics that do not experience excessive shrinkage, which is likely due to sintering of the preceramic precursors. This shrinkage greatly limits the geometrical accuracy; therefore machining is often required to achieve the necessary precision [1, 13]. From this, it can be seen that this technique has high relevance in the application of manufacturing silicon carbide that is suitable and desirable for use in nuclear reactors.

This technique albeit, relatively new in the means of manufacturing high yield ceramics, possesses some advantages over other similar techniques, such as chemical vapor deposition (CVD) and high temperature sintering [37]. This method only requires a controlled atmosphere inside the furnace. Also, the liquid polymer precursor that is utilized can be easily handled and stored for extended periods of time given the appropriate conditions. This process is also very environmentally friendly as the residual gases do not require any cleansing or purification. This method is dust-free which can make it attractive for processing radioactive elements such as plutonium and americium [37]. With previous understanding and appropriately designing and constructing the parameters that will ultimately result in an enhanced microstructure to minimize stresses and other qualities detrimental to the optimization of nuclear characteristics, this technique can prove promising.

The principal focus of this research investigation is to employ a pyrolysis based technique to fabricate a highly dense silicon carbide from a liquid polymer precursor through low

temperature and pressure annealing. In addition to the polymer infiltration method, it is anticipated that the addition of nano-sized metal particles will enhance the sintering behavior, material and mechanical properties of the processed silicon carbide via the pyrolysis method. The enhanced sintering behavior through the addition of metal nanoparticles is believed to occur through liquid phase sintering of the silicon carbide. Lastly, another processing technique, freeze casting, will be utilized to manufacture a rigid body with controlled porosity. This technique will allow for advantage knowledge on processing methods of silicon carbide that can ultimately be utilized in other applications. In addition, mechanical characterization through the use of hardness testing will become a benchmark on performance. X-ray diffraction is used to determine any reactions as well as asses the phases present in the materials that occur as a result the pyrolysis in the manufacturing process. Finally, any additional factors that affect the processing and manufacturing of polymer precursor derived silicon carbide are characterized and detailed as well as the practicability of this technique to process silicon carbide for nuclear-based applications, specifically to replace the current material, Zircaloy, as the primary material for cladding of a nuclear reactor.

4.0 EXPERIMENTAL PROCEDURE

4.1 POLYMER INFILTRATED PELLETS

The general procedure and methodology to generate the mechanically pressed silicon carbide pellets is described in detail in the following paragraphs. For any alterations in the fabrication process of the mechanically pressed pellets, the general procedure remains the same; however, small deviations and changes are noted as necessary.

4.1.1 Preparation for Mechanically Pressing Silicon Carbide Powder

Silicon carbide (~400 mesh particle size, ≥ 97.5% purity), purchased from Sigma Aldrich, is utilized in the production of these silicon carbide pellets. A pressing agent, polyethylene glycol (Carbowax Sentry, 900 NF, FCC Grade), is also used in order to provide structure for the silicon carbide particles to be held together in order to be molded into pellet form. This starting mixture contains 20 grams of the silicon carbide powder, which is crushed by mortar and pestle and sieved three times through 250 micron mesh, 50 mL of de-ionized water and 3% by weight of the polyethylene glycol all combined in a 250 mL beaker. The silicon carbide powder was mortar and pestle to ensure the particles are very fine for better recombination during the mechanical pressing. The mixture is then placed on a heating pad with a magnetic stirrer at low to medium heat for roughly four to six hours to allow for proper binding

of the silicon carbide powder. The heat is kept on low to medium to ensure that the powder does not become too dry for pressing into the pellet mold. If the powder becomes too dry, it will not take the shape of the pellet and will easily crumble and fall apart once removed from the mold.

Once the well mixed silicon carbide powder is cooled back down to room temperature, it is then taken to be pressed into a one (1.0) gram pellet, (~0.5 inch diameter, ~0.5 inch thick). After multiple trials and analysis of the one (1.0) gram pellet, the pellet size was decreased to one-half (0.5) of a gram. The reason for decreasing the size of the pellet was to ultimately increase the density and thus achieve greater mechanical behavior results. The 0.5 gram pellet has the dimensions of (~0.5 inch diameter, ~0.3 inch thick). To begin the pressing step, the silicon carbide powder is weighed out to approximately one-half (0.5) gram and then placed into a cylindrical molding dye-system, that can be seen in Figure 7, in order to compact the powder.

Figure 7 - Molding Dye Used for Pressing Silicon Carbide

Once the powder is in the cylindrical container, it is then placed under the pressing machine, a Carver Press, as seen in Figure 8, and pressed to 10,000 pounds. The pressing is done slowly in order to ensure good compaction of the pellet. The machine is held at 10,000 pounds for approximately 30 seconds and then slowly decreased until the cylindrical container can be taken from the press.

Figure 8 – Mechanical Pressing Machine for Compacting Silicon Carbide into Pellet Form

Once the molding dye is taken off the pressing machine and the pellet is carefully removed out of the molding dye, the pellet is placed in a graphite crucible in order to be annealed to transform the phase from amorphous to crystalline. Figure 9 displays the pre-annealed silicon carbide pellet once it was removed from the molding dye.

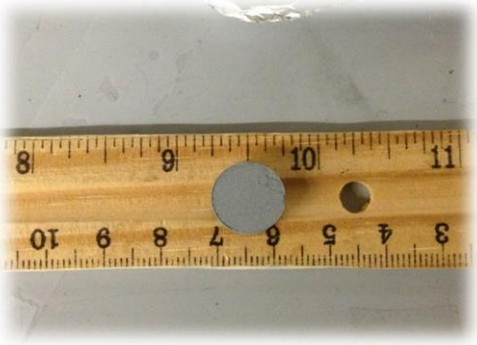

Figure 9 - Pre-Annealed Silicon Carbide pellet

4.1.2 Annealing of Silicon Carbide Pellets

Pellets are placed in a graphite crucible, which is then placed into a Webb 109 furnace, displayed in Figure 10. The crucible is then placed in the center of the furnace and the top of the

furnace is tightly sealed. The heating chamber is emptied by way of a vacuum pump then filled with argon gas to provide an inert atmosphere, thus to avoid any oxidation of pellets during the sintering phase. From here, the appropriate program is entered into the furnaces settings. For annealing, the first step is to heat the sample up to 500 degrees Celsius with a ramp rate of 15 degrees Celsius per minute. Once at 500 degrees Celsius, the temperature is held constant for 30 minutes. This is done to burn off the polyethylene glycol as well as the deionized water to ensure a more pure sample of silicon carbide. In case some polyethylene glycol and water still remain in the sample after holding the temperature at 500 degrees Celsius, the ramp rate to the final temperature, 1500 degrees Celsius, is lowered to 10 degrees Celsius per minute. This will remove any of the water or polyethylene glycol that was present after the first step in this process. After the final annealing temperature is reached, the program holds the chamber at this temperature for two (2) hours to ensure thermal equilibrium. Finally, the last step of the program is slowly cool back down to the initial starting temperature of approximately 20 degrees Celsius. A low flow rate of argon gas is kept inside the heating chamber during this process. The flow rate is dependent on keeping the pressure in the heating chamber as close to 0.0 mmHg as possible. However, a variation of +/- 2.5 mmHg is typically the range the pressure is kept between. To avoid any additional impurities or oxidation, the samples are left in the argon gas filled chamber until the next phase of this process is ready to commence.

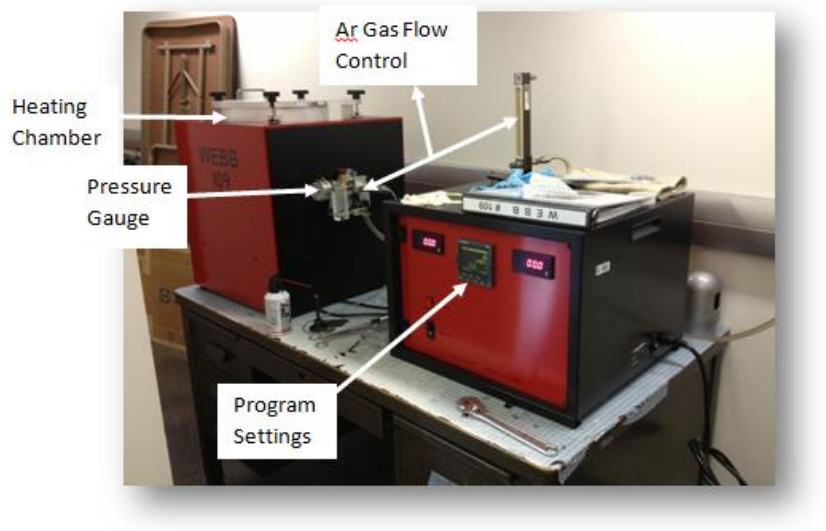

Figure 10 - Webb 109 Furnace Used for Annealing and Infiltration of Silicon Carbide Pellets

4.1.3 Infiltration of Silicon Carbide Pellets with Allylhydridopolycarbosilane (AHPCS)

The next phase is the polymer infiltration of the silicon carbide pellets. First, about 50-60 mL's of Allylhydridopolycarbosilane (AHPCS) is placed into a 250 mL Buchner funnel. After which, the pellets are carefully placed into the funnel, making sure there is no contact between any of the pellets. Ensuring that there is no contact between the pellets during the infiltration process allows for the polymer precursor to infiltrate without any discrimination in hopes of filling most of the pores. Once the pellets are submerged in the polymer, a vacuum line is connected to the funnel and air is continuously vacuumed out. This is done to infiltrate the pellets with the polymer, as the polymer is essentially pulled through the silicon carbide pellets. This process can be seen in Figure 11.

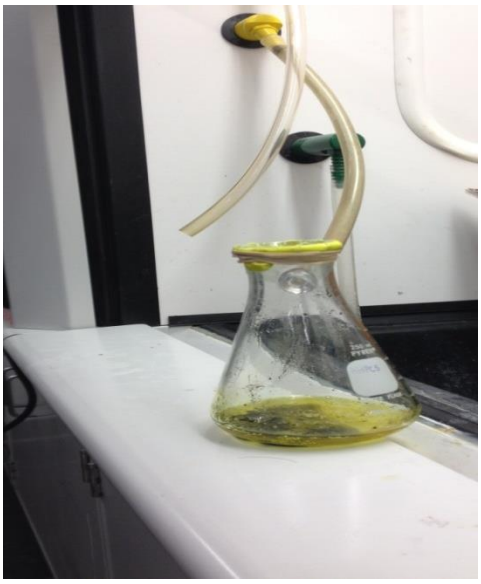

Figure 11 - Vacuum Infiltration of Silicon Carbide Pellets with AHPCS

The samples are under vacuum for approximately two to three hours to ensure that the polymer has infiltrated the pellets well enough and that no more polymer precursor can be infiltrated into the pellets. It is visually apparent at this time that there are no more bubbles present, which is a strong indicator that the polymer is being infiltrated into the pores of the pellets. Then from the vacuum filtration, the pellets are placed back in the graphite crucible and put in the heating chamber of the Webb 109 furnace. Again, vacuuming out the air and filling the heating chamber with argon gas to provide an inert atmosphere to avoid any oxidation.

Similar to the annealing phase, this pyrolysis stage has its own program on the furnace. There were several attempts to find the best program for the infiltration heating step of this process. Initially, the temperature was ramped 1 degree Celsius up to 900 degrees Celsius. This was a lengthy process, but it did give good density results that will be displayed in the results section. The next attempt at the heating step was to quickly ramp the temperature up to 900 degrees Celsius, where the ramp rate was 10 degrees per minute up to 900 degrees Celsius. This method did not provide as good density data as the first attempt; therefore this method was

neglected and determined to be inefficient at producing noteworthy results. According to Singh, a slow heating rate is known to favor the lower temperature curing of the polymer up to about 650 degrees Celsius. Then after this temperature the rate at which the temperature is increased does not greatly affect the curing of the polymer. This is very critical in filling the porosity of the material. Therefore, the next attempt, and ultimately the one that was found to provide the best results in terms of density and mechanical behavior, increased the temperature by 1 degree per minute up to a temperature of 650 degrees Celsius then up to 1200 degrees Celsius by 5 degrees Celsius per minute. Once at 1200 degrees Celsius, the furnace holds the temperature there for one-half hour after which, it is cooled back down to the initial temperature of the furnace. This infiltration process is completed for a total of four (4) times. It is visually apparent that after four (4) infiltrations that the maximum amount of polymer has infiltrated the silicon carbide pellets. In addition to the visual notification, a negligible mass and density increase was noticed when infiltrating for a fifth time. After each infiltration a bulk density calculation is recorded. Figure 12 shows the status of a four (4) time infiltrated silicon carbide pellet with AHPCS.

Figure 12 - 4 Time Infiltrated and Sintered Silicon Carbide Pellet

4.2 NICKEL NANOPARTICLE ADDITION

The silicon carbide pellets that were used in the experimentation with nickel nanoparticles were prepared in a similar fashion as described in detail in the previous section. After they were mechanically pressed, they were annealed following the same temperature profile, reaching a final temperature of 1500 degrees Celsius.

As previously mentioned, it is believed that the addition of metal nanoparticles will ultimately increase the mechanical as well as structural properties of the silicon carbide pellets. For the desired nuclear application, the chosen metal nanoparticles need to possess a low neutron absorption cross section in order to provide a stable neutron economy inside the core. Therefore, carbon coated nickel nanoparticles (20 nanometers, 99.9% purity), purchased from US Research Nanomaterials Inc. were utilized. The carbon thickness of the nickel nanoparticles was approximately 0.47 nanometers, according to the relation provided by US Research Nanomaterials as seen in Equation 7.

$$\text{Carbon Thickness} = (1/3)(\text{Particle Radius})(\text{Ni density}/\text{C Density})(\text{C wt\%})$$

$$\text{Carbon Thickness} = (1/3)(10\text{ nm})(8900/2267)(3.61\%)=0.47\text{ nm}$$

Equation 7 - Carbon Thickness on Nickel Nanoparticles

Even with the carbon coating of these nickel nanoparticles, they can experience rapid oxidation and become nickel oxide, therefore; they were only used inside an argon controlled atmosphere glove-box, (Protector Glovebox, Labconco), as seen in Figure 13. For the intentions of this part of the process, nickel oxide is not a desirable product in the process of manufacturing metal nanoparticle silicon carbide pellets, strictly nickel nanoparticles are the desired product in hopes of enhancing the mechanical properties of the silicon carbide based pellets.

Figure 13 - Glovebox Used for Infiltration of Nickel Nanoparticles

Therefore, by weight percent, nickel nanoparticles were carefully placed in Buchner funnels in combination with the polymer precursor, AHPCS. In the first Buchner funnel, 5% by weight nickel nanoparticles were added, while in the second Buchner funnel, 10% by weight nickel nanoparticles were added. These were added to the polymer precursor to ensure a more even distribution inside the silicon carbide pellet during the infiltration process. A more even distribution process is likely to increase the mechanical properties of the pellets. This is in opposition of where the nickel nanoparticles are freely scattered with no good distribution, which would likely result in local increased properties instead of increasing the total, overall properties.

To prevent any oxidation of the nickel nanoparticles, the Buchner funnels were placed inside the glove-box and then were infiltrated via vacuum filtration. Again, these pellets were submerged and vacuumed for roughly two to three hours to ensure that the polymer and nickel nanoparticles had filled the pores of the pellet. Once the vacuum filtration was complete, the pellets were loaded in a graphite crucible and placed directly into the Webb 109 furnace after being removed from the glove-box. This step was done quickly and efficiently to limit the amount of exposure to the air atmosphere.

Again, the furnace was filled with argon gas to ensure no oxidation during the pyrolysis process. These pellets were treated under the same temperature profile as above, where the temperature was slowly increased to 650 degrees Celsius by one degree per minute then increased to 1200 degrees Celsius by 5 degrees per minute. The same total number of infiltrations was kept constant for the AHPCS, 5% and 10% pellets, which was four. After the fourth infiltration, it was visually apparent that no more polymer precursor and nickel particles were infiltrating the silicon carbide pellet, as there were no bubbles present to represent infiltration.

4.3 POLISHING OF SILICON CARBIDE SAMPLES

Once the pellets have been infiltrated four times and have achieved an optimum density, they are prepared for the next phase where their mechanical properties are to be analyzed. To analyze their mechanical properties, their surface, as well as cross-section, must be polished so that the analysis is highly accurate. A smooth, finely polished surface provides better results than a rough, unpolished finish as this can lead to obscure and misleading data. To analyze the cross-section of the silicon carbide pellets, they were cut using a diamond blade saw (Norton Abrasives).

Therefore, to polish the pellets were individually cast in a polymer mold, (Epoxicure Epoxy Resin, Buehler Co.) and hardener (Epoxicure Epoxy Hardener, Buehler Co.) in a ratio of 5 parts resin to 1 part hardener. Once this was properly mixed, minimizing the amount of air bubbles, it was carefully poured over the silicon carbide pellets that resided in sample cups. The

pellets are cast in the mold for 24 hours to ensure that the resin and hardener has solidified and the pellets are securely fastened in the polymer.

From here, with the pellet secured in the mold, it is placed into a disk that holds six molds for polishing. This disk securely holds the molds and allows for even polishing of all the samples, which is placed securely onto (Ecomet 4, Buehler Co.) with an automated head attachment (Automet 2, Buehler) as seen in Figure 14. Once the disk is fastened in place on the mechanical polisher, the correct cloth is selected. The automated head has the option to rotate both clockwise as well as counter-clockwise. For the following polishing procedure, both directions were utilized to polish the samples.

Figure 14 - Ecomet 4 Polishing Machine

For this grinding and polishing process, there are four cloths that are utilized. The first cloth is a 45 micron silicon carbide based cloth, Ultra-Prep Metal Bonded Diamond from Buehler. This cloth is meant to prepare the pellet for the finer cloths that will be used in the following steps. This 45 micron cloth is rough and abrasive and begins to smooth out the surface of the pellet casted in the polymer mold. It also is meant to make the pellet surface more level for

a more even polishing during the later stages of this process. This cloth is crucial because it is very difficult to polish silicon carbide as it possesses a high hardness value. Therefore, with this cloth the surface of the pellet can be smoothed out in order to prevent any damage to the following cloths. If the surface of the pellet is not smooth, the following cloths would rip and have tears through them and render the polishing of the pellet useless. The settings for this cloth have the polishing machine wheel was spinning at 150 revolutions per minute (RPM) rotating in the counter-clockwise direction of the pellets and a force load of 28 lbs being applied. Typically, this phase of the grinding and polishing takes approximately 10 to 20 minutes to complete. The phase is kept short in order to prevent any grains in the silicon carbide microstructure from being pulled out.

Once the top layer has been smoothed and leveled, the next cloth is placed on the wheel of machine. This cloth is 9 micrometers in size, with the name Trident from Buehler, and is used in unison with 9 micrometer Meta-Di Polycrystalline Diamond Suspension. In addition to the solution, a 9 micrometer diamond paste, Ultra Diamond Paste, is placed on the surface of the pellet. This diamond paste is used to help create a fine, glossy polish on the pellet. The settings on the polishing machine wheel for this cloth is 120 RPM's rotating in the clockwise direction as the pellets and a force load of 27 lbs being applied. For this part of the polishing process, it takes approximately 60 minutes to produce a nice sheen on the surface of the pellets. Once the pellets surface begins to possess a shiny, glossy look the next cloth can be used.

The next cloth to be used is 3 microns in size, with the name Ultra from Buehler, which again is used with a 3 micron solution, Meta-Di Supreme Polycrystalline Diamond Suspension and a 3 micron diamond paste, Ultra Diamond Paste. Here, the glossiness of the pellets is to be increased and at the end it should be possible to see a reflection on the pellets surface. For this

cloth, the wheel of the machine is spinning at 120 RPM's rotating in the counter-clockwise direction of the pellets with a force of 25 lbs being applied. The three micron phase often takes upwards of an hour and a half to successfully polish the surface without any flaws.

Finally, the last cloth to be used is a submicron, by the name of Chemomet from Buehler, cloth used in combination with a submicron polishing solution, MasterMet2 Non-Crystallizing Colloidal Silica Polishing Suspension. This phase is to simply make sure the pellet is smooth and is as glossy as it can be. Therefore, the settings on the polishing machine in this step are 100 RPM's rotating in the clockwise direction as the pellets and a force load of 25 lbs being applied. Since this phase is merely meant to ensure the most enhanced luster of the surface it is ran until it is visually apparent that the surface cannot become any glossier. The samples were cleaned using an ultrasonic bath for roughly 3 minutes once changing to a different size diamond cloth and paste in order to avoid any cross-contamination from the different polishing materials. This procedure has proven to show good polishing results of silicon carbide pellets as they can then be analyzed for their mechanical and microstructural properties. Having a fine, polished surface allows for more accurate results as the microstructure can be better analyzed by the techniques of scanning electron microscopy (SEM), optical microscopes as well as nano-indentations.

After the final phase of the polishing process, the pellets were ready to be analyzed under the SEM (XL-30 FEG, Philips). Since the samples are silicon carbide they need to be coated with palladium to enhance the results of the SEM and to avoid and charging spots when analyzing the pellet. The pellets were coated with a thin coating through the use of a magnetron sputter coater (Model 108 auto, Cressington Scientific Instruments, Ltd.). The samples were coated for approximately 60 seconds, which proved to be thick enough when analyzing under the SEM.

4.4 FREEZE CASTING OF SILICON CARBIDE

In order to produce the desired directional pores in the silicon carbide pellets, the freeze cast method was employed. Here, silicon carbide powder (~400 mesh particle size, ≥ 97.5% purity), purchased from Sigma Aldrich, is utilized in combination with deionized water, a dispersion agent Duramax D-3005 (Dow Chemical Company, Philadelphia, Pennsylvania) and polyethylene glycol (Carbowax Sentry, 900 NF, FCC Grade). To prepare the recipe for freeze casting of silicon carbide, 25 volume percent silicon carbide powder is mixed with 0.01% Duramax D-3005, polyethylene glycol at 4 weight percent and remainder by deionized water. This solution is then stirred continuously for 24 hours to ensure proper mixing of all components in the recipe.

As the solution is mixing, the freeze casting equipment is setup. For the initial experiment, a small piece of rubber tubing, length approximately 4 centimeters with a diameter roughly 2 centimeters, is placed over a circular, aluminum mold as seen in Figure 15. The mold is placed inside a plastic container, to where liquid nitrogen is poured into in order to create the cold atmosphere required to freeze cast the solution. For safety purposes, an outside containment of Styrofoam is used, which can also been seen in the figure.

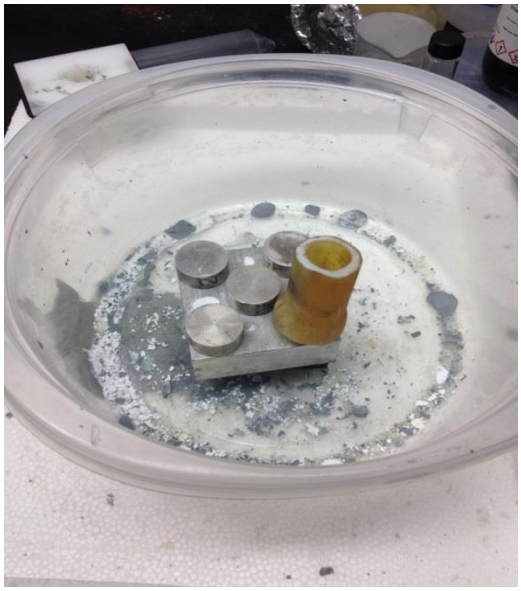

Figure 15 - Initial Freeze Cast Sample Holder

After the equipment is properly setup and the solution is well mixed, the solution is brought directly to the plastic container that is supporting the aluminum mold and plastic rubber tubing. The silicon carbide solution is poured directly into the rubber tubing hole and then without much delay, the liquid nitrogen is poured into the plastic container surrounding the aluminum mold. The liquid nitrogen freezes the tubing and the solution inside creating unidirectional pore channels in the freeze cast mold of silicon carbide. After roughly 8 to 10 minutes in the liquid nitrogen bath, the tubing is removed and the solid mold of silicon carbide is placed directly into a freeze dryer, (FreeZone 2.5, Labconco) where the ice can be sublimed and essentially removed from the mold. The freeze dryer is under vacuum at -50 degrees Celsius and a pressure of 1.236 Torr. The solid pellets of silicon carbide are left under these conditions for approximately 24 hours to ensure that all the ice has sublimed and that the mold will not melt once removed from the freeze dryer.

After 24 hours of freeze drying, the solid pellets of silicon carbide are removed and then placed in a graphite crucible to be sintered. The program for sintering the silicon carbide pellet is

as follows: the first step is to heat the sample up to 500 degrees Celsius with a ramp rate of 15 degrees Celsius per minute. Once at 500 degrees Celsius, the temperature is held constant for 30 minutes. This is done to burn off the polyethylene glycol to ensure a more pure sample of silicon carbide. In case some polyethylene glycol still remains in the sample after holding the temperature at 500 degrees Celsius, the ramp rate to the final temperature, 1500 degrees Celsius, is lowered to 10 degrees Celsius per minute. This will remove any of the polyethylene glycol that was present after the first step in this process. After the final annealing temperature is reached, the program holds the chamber at this temperature for two (2) hours to ensure thermal equilibrium. This is all performed under an argon ambience at a flow rate of approximately 3 cubic feet per minute (CFM). As it can be seen, this process is quite similar to the annealing step of the mechanically pressed silicon carbide pellets.

After the samples have been annealed to 1500 degrees Celsius and have cooled down to room temperature, they are taken from the furnace and placed into a funnel where they can be vacuum infiltrated with the same polymer precursor, AHPCS, similar to the method used for the silicon carbide pellets that were mechanically pressed into shape. These freeze cast silicon carbide pellets are vacuum infiltrated for roughly two hours. Once this process is complete, they are placed back into the graphite crucible and into the furnace. Again, the temperature profile used is identical to the one used previously. The temperature is slowly ramped, 1 degree Celsius per minute, up to 650 degrees Celsius. Here the temperature dwells for roughly half an hour then continues to 1200 degrees Celsius via a ramp rate of 5 degrees Celsius per minute. This infiltrate process is completed a total of four times, similar to the previous method in order for comparison and understanding. After each infiltration, a density is taken via the Archimedes method as these pellets are not cylindrical.

The initial method rendered pellets that were not cylindrical or any other shape that a volume equation could be applied in order to calculate the bulk density. Therefore, a revised mold was used that allowed for a more cylindrical shape of the freeze cast silicon carbide. However, after infiltrating with the polymer precursor, the cylindrical shape was altered and thus a bulk volume calculation could not be obtained. This mold can be seen in Figure 16.

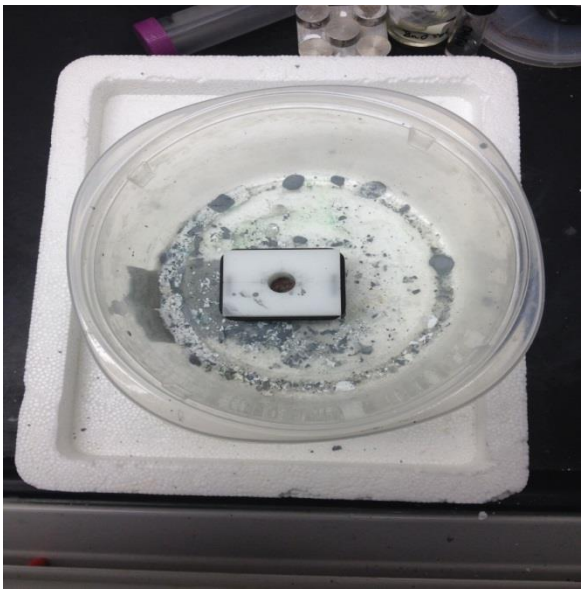

Figure 16 - Revised Mold for Freeze Cast Method

The same methodology was applied in that the silicon carbide solution was poured directly into the center hole, then liquid nitrogen was poured inside the container, freezing the silicon carbide solution in a unidirectional fashion. The pellet was carefully removed from the center hole and placed in the liquid nitrogen until it was ready to be transfer to the freeze dryer, where again the ice would be sublimed. Once the ice was completely sublimed, the silicon carbide pellets were taken from the freeze dryer, placed in a graphite crucible and prepared for annealing to 1500 degrees Celsius following the same pattern as before. After annealing, the samples were infiltrated with the polymer precursor, AHPCS, and annealed to 1200 degrees

Celsius following the same temperature profile as previously stated. This was done a total of four times. After each infiltration, a density of the sample was recorded.

5.0 RESULTS AND CHARACTERIZATION

In order to quantitatively and qualitatively assess the performance of the mechanically pressed silicon carbide pellets as well as the freeze casted samples, their mechanical properties must be characterized as well as validated. To properly characterize the properties, several tests must be performed in order to accurately evaluate the pellets. The testing of the pellets is crucial to understanding and characterizing their performance under certain situations that may arise where the application of the silicon carbide pellets is applicable, for instance, the fuel cladding in a nuclear reactor or other potential structural components.

These tests include but are not limited to; density calculations, x-ray diffraction measurements, analysis under optical microscopes, scanning electron microscopes, as well as determination of the hardness value from micro-indentations made on a polished surface. In addition to these testing applications, characterizing the pellets by way of nano-indentation, compression testing, transmission electron microscopy as well as testing their thermal conductivity is on the list of future testing procedures to accurately analyze the silicon carbide pellets to gain a further understanding of the processed pellets. All of these tests are essential in facilitating the intellectual capacity of how these silicon carbide pellets will perform due to studying the intricate details of the microstructure.

The following sections detail the specific results obtained from analyzing the silicon carbide pellets, the nickel nano-particle infiltrated pellets as well as the freeze casted samples.

These results were obtained from analyzing the samples at the University of Pittsburgh, with the specified equipment as stated. The testing of the samples and ultimately the results were repeated multiple times to ensure validity and reasonability of the obtained values for each test of the samples.

5.1 CRYSTALLOGRAPHIC CHARACTERIZATION

X-ray diffraction is a powerful technique used to identify phases through comparison with data from known structures. It quantifies changes in the cell parameters and helps to further understand the crystal unit cell orientation. X-ray diffraction patterns were obtained through the use of a Phillips Analytical X-Ray Machine that used a copper k-alpha value of 1.54 angstroms. X-ray patterns were obtained after the initial annealing to 1500 degrees Celsius and each subsequent infiltration to 1200 degrees Celsius. This was a crucial testing parameter due to the fact that one of the initial assumptions was that the phase was crystalline and not amorphous. X-ray diffraction would assist in further differentiating the phases after annealing.

5.1.1 Silicon Carbide Pellets

Seen in Figure 17 is the XRD pattern of the silicon carbide pellets after annealing to 1500 degrees Celsius with no infiltration, whereas in Figure 18 shows the XRD of the fourth and final infiltration of the silicon carbide pellets that had a temperature profile up to 1200 degrees Celsius. The XRD patterns after the first, second and third infiltrations are very similar to that of the fourth infiltration and thus why only the fourth infiltration XRD pattern is shown. Therefore,

since the first, second and third XRD patterns are similar to the fourth, it is reasonable to believe that there are no apparent phase changes during the PIP method used to manufacture the silicon carbide pellets. When comparing the 1500 degree Celsius profile to that of the 1200 degree profile, it can be seen that additional peaks are present after infiltration. The additional peaks can be a result of an unsuppressed orientation that was causing destructive interference when the 1500 degree annealed pellets were analyzed. Further analysis is required to precisely determine the cause of these additional peaks, whether it is crystallinity or a processing parameter that is causing this effect.

Having this information allows for the conclusion that at the given temperature of 1200 degrees Celsius there is no phase change, which is also understood through the literature. In addition, it is also critical to know due to the fact that if there was a phase change present during the pyrolysis at 1200 degrees Celsius, that would likely indicate some sort of additional reaction or formation is occurring during the pyrolysis after the samples have been vacuum infiltrated with AHPCS. However, as stated, there is no ostensible phase change present during each stage of the pyrolysis and infiltration. The silicon carbide peaks, as seen in the following X-Ray diffraction patterns, were indexed by using a primitive, hexagonal silicon carbide structure with the “a” cell parameter being equal to 3.095 and the “c” cell parameter being equail to 15.17. From the standard diffraction peak analysis, there was no “b” cell parameter provided. As it can be seen from the diffraction pattern, some peaks possess two miller indices; however, through calculations, both indices for each peak are equivalent and are accurately represented.

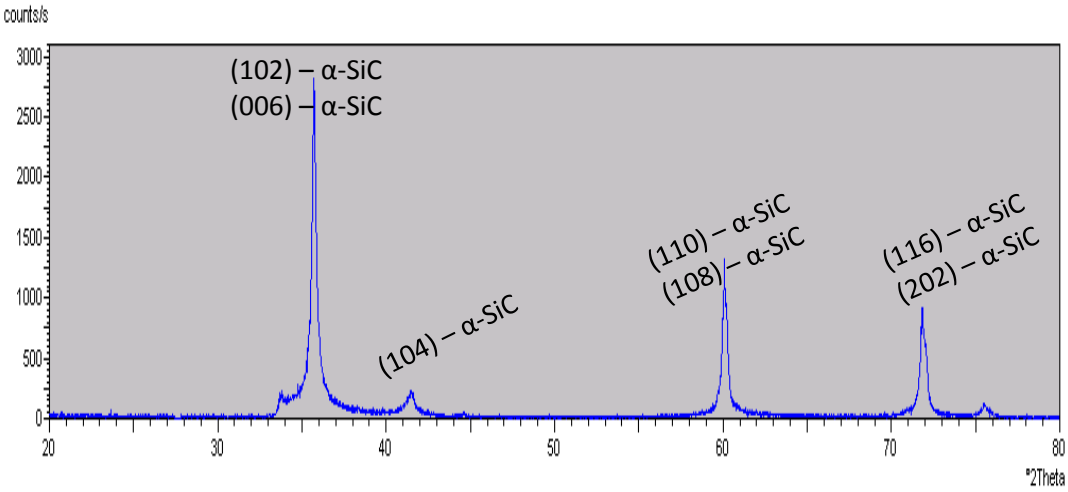

Figure 17 - XRD of 1500 Degree Annealed Silicon Carbide Pellet

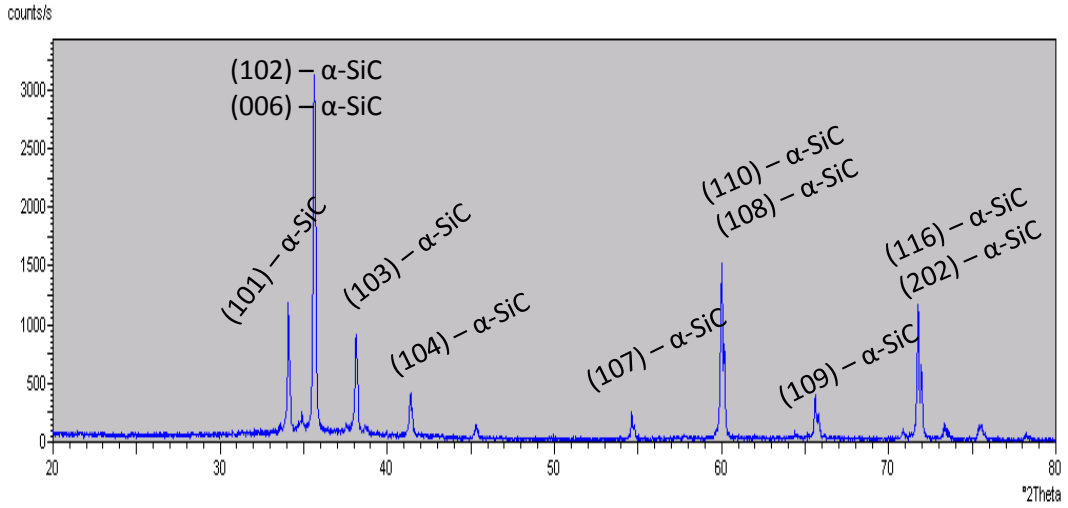

Figure 18 - XRD of Four Time Infiltrated Silicon Carbide Pellet

All of the peaks present in the four times infiltrated pellet are a strong indicator that the sample is silicon carbide when compared to standard XRD patterns of silicon carbide.

5.1.2 Nickel Nanoparticle Silicon Carbide Pellets

The next pellets to be analyzed under the XRD were the nickel nanoparticle infiltrated silicon carbide pellets. Since XRD is not entirely dependent on the weight amount of particles in a given sample and merely only what atoms are present, only the 5 weight percent nickel nanoparticle

infiltrated pellets were analyzed under the x-ray machine. For verification purposes, the 10 weight percent nickel nanoparticle infiltrated pellets were analyzed under the same conditions, resulting in an expected, similar pattern as the 5 weight percent pellets. The results from the 5 weight percent nickel nanoparticle XRD pattern can be seen in Figure 19. Again, the first, second and third infiltrations resulted in similar XRD patterns and hence why only the fourth and final XRD infiltration of the nickel nanoparticles is shown. As a note to mention, again these XRD patterns of the nickel nanoparticle silicon carbide pellets were those following the temperature profile up to 1200 degrees Celsius.

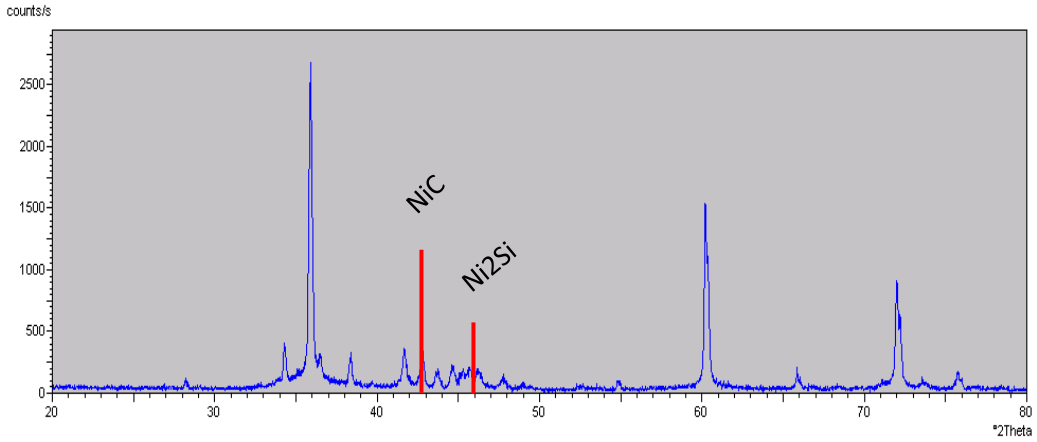

Figure 19 - Four Time Infiltrated, 5 wt% Nickel Nanoparticle Pellet

When comparing the nickel nanoparticle XRD pattern to the AHPCS four times infiltrated pattern, it can be ascertained that once again additional peaks are present. However, in the nickel nanoparticle pattern, the additional peaks are not as strong as they were in the AHPCS pattern. When analyzing standard nickel carbide XRD patterns, it is believed that nickel carbide is present around the 42 to 45 2-theta region on Figure 19. This is a good indication that the nickel nanoparticles are combining with carbon to form a strong bond together. The reaction is likely to be that of exothermic in nature, which prospectively enhances the sintering behavior of the silicon carbide pellets as a whole and thus has allowed for a higher density. This formation of

nickel carbide is believed to be true due to the binding energy of nickel carbide being approximately 3.95 eV, which means it forms a bond easier than nickel silicide, about 3.30 eV or silicon carbide, 2.75 eV.

Additionally, there is a peak present in the range of 48 2-theta. After analyzing standard diffraction peaks of silicon carbide and silicon nickel, as well as their respective phase diagrams, there is the possibility of Ni_2Si being formed through this process. Previous studies have determined the first silicide to form when nickel interacts with silicon carbide is that of delta-Ni_2Si; therefore, it is believed that this product is produced from the interaction of nickel nanoparticles and silicon carbide. When analyzing the phase diagram of nickel and silicon, it can be seen that delta- Ni_2Si is formed around the processing temperature of 1200 degrees Celsius. Also, when analyzing the phase diagram, seen in Figure 20, it can be ascertained that liquid can form well below the processing temperature, at approximately 1000 degrees Celsius. From this, it is believed that liquid phase sintering can occur through the addition of nickel nanoparticles. These two different areas of crucial to note as each of these newly formed compounds possess different properties that can greatly affect the desired end goal of the performance of the pellets. In addition to the crystallographic characterization, EDS was performed; however, the resolution was poor and further testing using this method need to be applied.

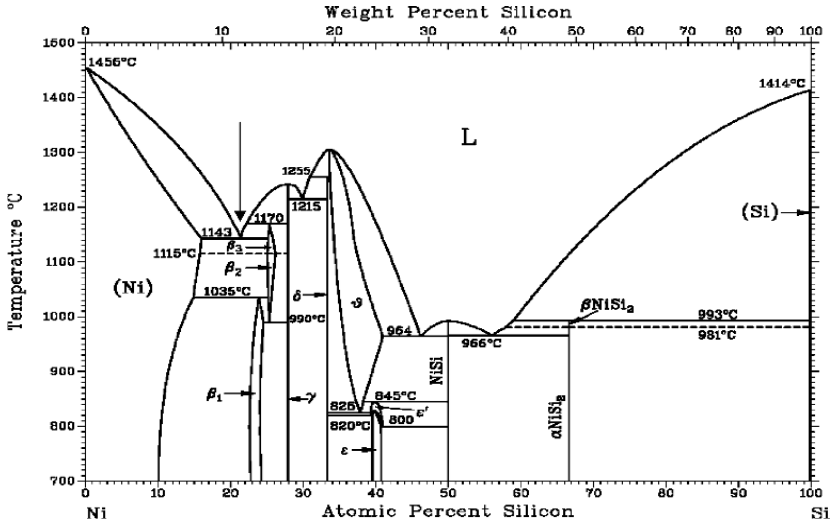

Figure 20 - The Ni - Si Phase Diagram[40]

5.2 DENSITY

An important characteristic to measure and quantify of the silicon carbide samples is density. As previously described, the PIP method, up until now, has failed to result in any highly dense silicon carbide samples, even after multiple infiltrations of the AHPCS polymer precursor. It is believed that through understanding of previous experiments performed by researchers, a more, highly dense silicon carbide sample can be achieved.

5.2.1 Infiltration Density Measurement

To measure the bulk density of the polymer infiltrated silicon carbide and nickel nanoparticle pellets, it was first assumed that the pellet was perfectly cylindrical in order to apply the volume equation of a cylinder. In order to calculate the volume, a precise and accurate measurement of the silicon carbide pellet needed to be obtained. This was done by using a caliper that was

accurate to 0.05 millimeters. The thickness and diameter of the silicon carbide pellet were obtained after each annealing step of the process. This was done to account for any volume change that was to occur during the pyrolysis and to ensure validity of the density after each infiltration. Now, with the volume calculated, the mass of the silicon carbide was obtained by weighing the pellet on a Mettler Toledo AC 104 weighing balance. The accuracy of this machine 0.001 grams. Again, after each infiltration, the weight of the silicon carbide pellet was obtained in order to properly calculate the bulk density. From here for each step of the process, the mass was divided by the volume and then recorded correspondingly.

5.2.2 Polymer Infiltrated Pellets

Initially, the temperature profile for the infiltration steps was set at a ramp rate of 1 degree Celsius per minute up to 900 degrees Celsius. For this set of data, the silicon carbide powder was not exposed to the mortar and pestle to reduce the size of the starting powder. Rather, these samples were strictly created from the powder obtain from Sigma-Aldrich. The results of the density from this temperature profile can be seen in Table 2.

Table 2 - 900 Degrees Celsius with Ramp Rate of 1 Degree per Minute

	Annealed	1^{st} Infiltration	2^{nd} Infiltration	3^{rd} Infiltration	4^{th} Infiltration
Density (g/cm^3)	2.365	2.681	2.825	2.972	3.028
% Silicon Carbide	73.90	83.52	88.00	92.59	94.33
Mass Increase (g)		0.0651	0.0285	0.0179	0.010
Std. Deviation of Density	0.0085	0.0062	0.0098	0.0112	0.0124

By changing the final temperature up to 1200 degree Celsius, it is believed, through previous research, that the density can be increased. With this temperature profile, the temperature is increased by 1 degree per minute up to 650 degrees Celsius, where it dwells for approximately one half hour, and then it is heated to its final temperature of 1200 degrees Celsius with a ramp rate of 5 degrees per minute. Therefore, the results of this alteration can be seen in Table 3. As it can be seen from Table 3, the density does increase by changing the ultimate temperature the silicon carbide pellets are exposed to during the infiltration process.

Table 3 - 1200 degree Celsius Temperature Profile

	Annealed	1^{st} Infiltration	2^{nd} Infiltration	3^{rd} Infiltration	4^{th} Infiltration
Density (g/cm^3)	2.390	2.709	2.8655	2.997	3.045
% Silicon Carbide	74.25	83.95	89.27	92.98	94.85
Mass Increase (g)		0.0652	0.0292	0.0182	0.0115
Std. Deviation of Density	0.0067	0.0059	0.0122	0.0125	0.0129

The next attempt to increase density was to sieve the starting silicon carbide particles. It is known that the better packing a material has, a greater density can be achieved. This is an attempt to reduce the amount of open space between the silicon carbide particles. Therefore, by sieving the starting silicon carbide particles it is believed that better packing can be obtained thus resulting in a higher density. The silicon carbide particles were sieved then mortar and pestled three consecutive times in order to achieve fine starting particles. For completeness, silicon carbide pellets that were sieved were exposed to all previous temperature profiles. Table 4 shows the sieved silicon carbide pellets under the temperature profile of 900 degrees Celsius. As where Table 5 displays the results obtained when the sieved silicon carbide pellets were sintered under

the 1200 degrees Celsius temperature profile. As it can be deduced from these tables, an increase in density was achieved as predicted when reducing the starting powder size by way of mortar and pestle.

Table 4 – Sieved Pellets, 900 Degree Temperature Profile

	Annealed	1st Infiltration	2nd Infiltration	3rd Infiltration	4th Infiltration
Density (g/cm^3)	2.371	2.689	2.832	2.979	3.040
% Silicon Carbide	73.86	83.76	88.22	92.80	94.70
Mass Increase (g)		0.0632	0.0271	0.0168	0.0098
Std. Deviation of Density	0.0062	0.0074	0.0095	0.0128	0.0126

Table 5 – Sieved Pellets, 1200 Degree Temperature Profile

	Annealed	1st Infiltration	2nd Infiltration	3rd Infiltration	4th Infiltration
Density (g/cm^3)	2.399	2.712	2.875	3.002	3.075
% Silicon Carbide	74.73	84.49	89.59	93.52	95.79
Mass Increase (g)		0.0657	0.0287	0.0185	0.0102
Std. Deviation of Density	0.0075	0.0082	0.0101	0.0105	0.0111

5.2.3 Nickel Nanoparticle Silicon Carbide Pellets

The next alteration that was made was the addition of nickel nanoparticles to the AHPCS polymer precursor liquid. The addition of nickel nanoparticles is believed to aid in the densification of the silicon carbide pellets. These nanoparticles are believed to have an effect on

the sintering behavior. It is believed that liquid phase sintering occurs through the addition of these nanoparticles. This will be further developed through the use of scanning electron imagery. In addition to the liquid phase sintering, the nickel particles likely interact with silicon carbide particles, which may also enhance the densification of the pellets. This is due to the previous experiments that were performed where the interactions of nickel and silicon carbide were studied. It was shown that the nickel diffuses into silicon carbide, which then the silicon carbide decomposes and reacts with nickel to form silicides and free carbon [41, 42]. Seen in Figure 21, is the backscattered electron image of the interface interaction of nickel and silicon carbide. Here it can be seen that the first silicide to form is Ni_2Si.

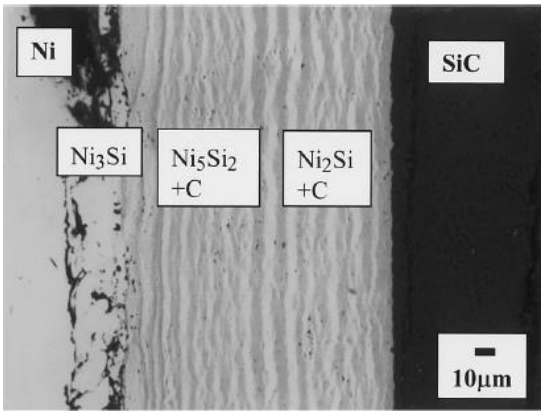

Figure 21 - Backscattered Electron Image of SiC/Ni reaction couple [42]

The formation of Ni_2Si is exothermic in nature and was predicted through previous studies. In addition to the formation of Ni_2Si, as seen by the crystallographic characterization, there was a peak for nickel carbide. The formation of nickel carbide would also be exothermic in nature. Through the creation of both of these products, it is likely they enhanced the sintering behavior. It is important to note two major differences between previous studies and the experiment performed is that solid nanoparticles were used as opposed to films in previous studies. It is believed that these solid nanoparticles can have a stronger reaction than films. Also, the nickel nanoparticles were added to the polymer precursor, where the silicon carbide bonds are not

strong yet. Therefore, these two differences are two potential reasons why nickel carbide formation was seen in this experiment as opposed to previous studies. Since it was discovered that increasing the final temperature to 1200 degrees Celsius provided the highest density of non-nanoparticles, it was decided that these nanoparticle infiltrated pellets would be taken to that temperature and not 900 degrees Celsius.

To determine the effect of the nanoparticles, two different percentages of nanoparticles were used. The two percentages, by weight, were 5 and 10 and added separately to two different flasks containing AHPCS. These two percentages were chosen due to only a maximum amount of metal nanoparticles can be added to silicon carbide matrix before the beneficial effects reach a climax. Due to the fact that these nanoparticles can be easily oxidized, they were infiltrated inside a Labconco Protector Series Glovebox in order to prevent any oxidation, since that is an undesirable consequence. The pellets were submerged in the AHPCS with the nickel nanoparticles, which were then infiltrated for the same time duration as the non-nanoparticle AHPCS pellets, about two to three hours. The theoretical density of the nickel nanoparticle silicon carbide pellets should be approximately the same as standard silicon carbide. The high surface area to volume ratio of the nanoparticles allows for a strong driving force for diffusion. The results of the 5 and 10 percent nickel nanoparticle infiltrated pellets can be seen in Table 6 and Table 7, respectively.

Table 6 - 5 wt% Nickel Nanoparticles, 1200 Degree Temperature Profile

	Annealed	1st Infiltration	2nd Infiltration	3rd Infiltration	4th Infiltration
Density (g/cm^3)	2.406	2.742	2.908	3.022	3.095
% Silicon Carbide	74.95	85.42	90.59	94.14	96.51
Mass Increase (g)		0.0692	0.0348	0.0197	0.0135
Std. Deviation of Density	0.0069	0.0071	0.0101	0.0103	0.0115

Table 7 - 10 wt% Nickel Nanoparticles, 1200 Degree Temperature Profile

	Annealed	1st Infiltration	2nd Infiltration	3rd Infiltration	4th Infiltration
Density (g/cm^3)	2.387	2.751	2.928	3.025	3.112
% Silicon Carbide	74.36	85.70	91.21	94.24	96.94
Mass Increase (g)		0.0713	0.0352	0.0211	0.0145
Std. Deviation of Density	0.0052	0.0088	0.0095	0.0100	0.0101

Again, in an attempt to increase the density of these nickel nanoparticle pellets, the starting powder sieved and exposed to the mortar and pestle and repeated three times. As with the previous sieving, the same sieve was utilized for this part. It is the belief that better compaction will allow for greater densification, as seen with just the silicon carbide pellets. The temperature profile used was the 1200 degree profile, due to the fact that it provided the best densification results. Therefore, with the addition of the nickel nanoparticles, having the silicon carbide powder sieved and utilizing the 1200 degree temperature profile, the highest densification of these pellets should ensue. The results of the 5 and 10 weight percent nickel nanoparticle silicon carbide pellets can be seen in Table 8 and Table 9, respectively.

Table 8 - 5 wt% Nickel Nanoparticles, 1200 Degree Profile, sieved

	Annealed	1st Infiltration	2nd Infiltration	3rd Infiltration	4th Infiltration
Density (g/cm^3)	2.419	2.752	2.923	3.037	3.117
% Silicon Carbide	75.35	85.73	91.21	94.59	97.12
Mass Increase (g)		0.0711	0.0360	0.0206	0.0156
Std. Deviation of Density	0.0053	0.0057	0.0096	0.0094	0.0101

Table 9 - 10 wt% Nickel Nanoparticles, 1200 Degree Profile, sieved

	Annealed	1st Infiltration	2nd Infiltration	3rd Infiltration	4th Infiltration
Density (g/cm^3)	2.399	2.760	2.941	3.049	3.123
% Silicon Carbide	74.70	85.99	91.63	95.00	97.50
Mass Increase (g)		0.0741	0.0368	0.0228	0.0152
Std. Deviation of Density	0.0047	0.0082	0.0082	0.0092	0.0092

In comparison to the non-sieved nanoparticle silicon carbide pellets, the sieved pellets were able to reach a slightly higher density, albeit again, not a substantial amount, but nonetheless, an increase was noticed. Figure 22 displays the non-sieved pellets with the number of infiltrations on the X-axis and the percent silicon carbide on the Y-axis. As where, Figure 23 shows the percentage of silicon carbide as a function of the number of infiltration of the sieved pellets. In these figures, the AHPCS-only silicon carbide results are included for completeness and comparative purposes.

Therefore, from the results presented on density, highly dense silicon carbide samples were successfully achieved through the use of the polymer precursor, AHPCS. These results are

higher than previous reports have indicated by rough 5 to 10 percent. This is quite a significant increase and one that should be noted due to the desire to create dense silicon carbide under low pressure and temperature annealing with minimal size change during the process. The comparison between the shrinkage, on a volume basis, and density for the sieved, AHPCS-only infiltrated sample can be seen in Figure 24; whereas the same comparison can be seen for the nickel nanoparticles in Figure 25.

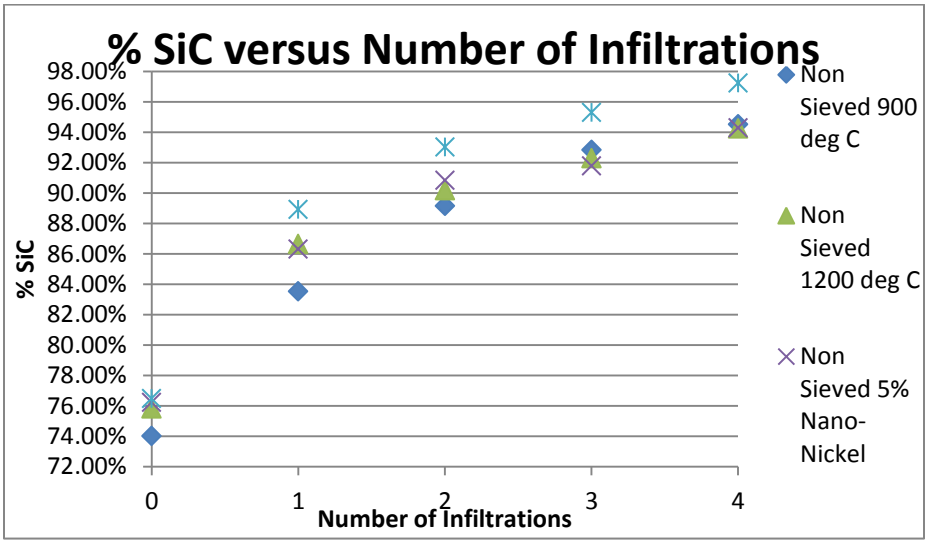

Figure 22 - Non-Sieved, Density versus Number of Infiltrations

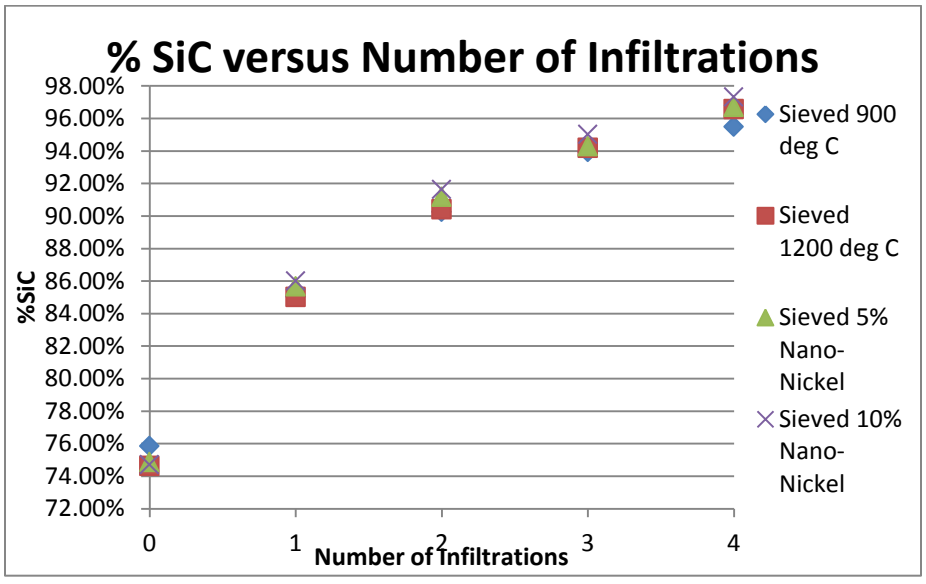

Figure 23 - Sieved, Density versus Number of Infiltrations

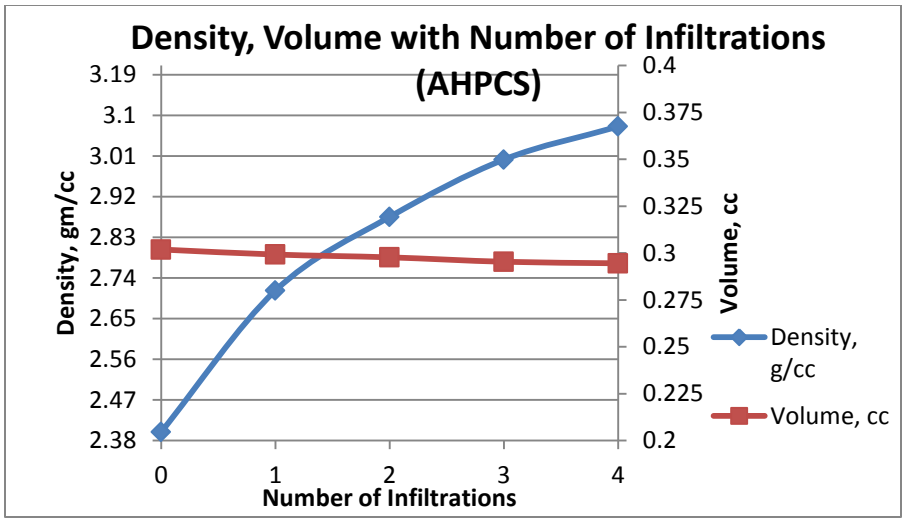

Figure 24 - Density, Volume vs Infiltration Steps (AHPCS)

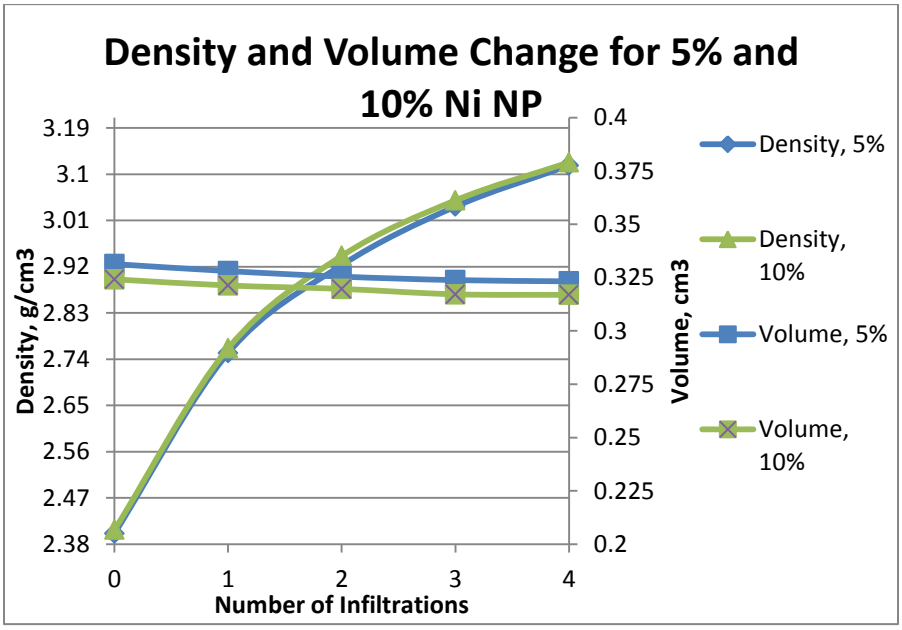

Figure 25 - Density, Volume vs Infiltration Step (Ni NP's)

5.3 SCANNING ELECTRON AND OPTICAL MICROSCOPE IMAGES

Scanning electron microscope (SEM) images are essential to gaining a more in depth knowledge and understanding of the microstructure of a material, while optical microscope images can give

a rather quick view of the surface of the polished sample and have a limited depth they can adhere to. Both techniques are useful to properly characterizing samples, as they both have advantages and disadvantages. Prior to being examined under the SEM and optical microscope, the pellets were finely polished in order to more accurately assess the microstructure. Seen in Figure 26, is a cross-sectional view of a silicon carbide pellet that was cut in half with a diamond saw from Saint Grobain, where in Figure 27 is a topical view of a silicon carbide pellet that was not cut in half, rather just polished on the surface. Both of these images are of the four time infiltrated silicon carbide pellets with AHPCS.

These images were both taken from the use of the SEM as opposed to the optical microscope. In essence, the optical microscope images would result in similar images of the surface and cross-section of the polished silicon carbide pellets. From the cross sectional image it can be seen that there are minimal open pores that did not successfully get filled with the polymer precursor. These open gaps, or dark spots, result in a less dense sample and since these are few in number and do not appear to be very large in size, the density achieved is within reason according to these findings from the SEM. The topical view of the polished silicon carbide pellet is also very important and it can be seen that again, not too many open pores remain after the four infiltrations with AHPCS. Having the cross-sectional view result is held in a slightly higher regard as opposed to the topical view due to the cross sectional view having a greater resemblance of the entire sample from a more mechanical property based point of view.

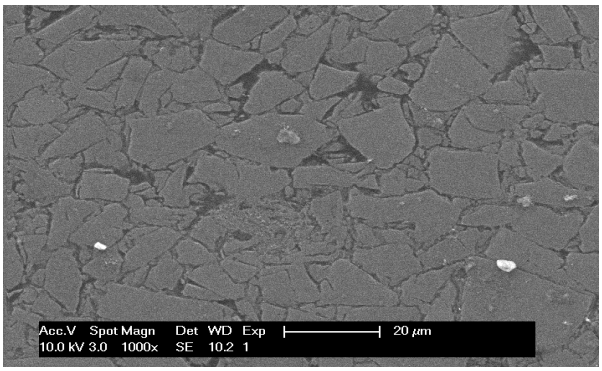

Figure 26 - Cross-Sectional View of Silicon Carbide Pellet

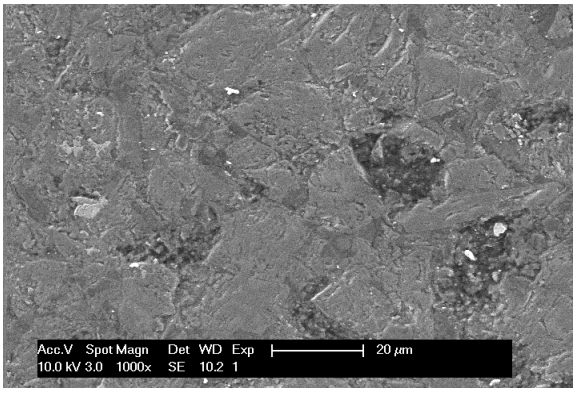

Figure 27 - Topical View of Silicon Carbide Pellet

The next analysis of the pellets was to polish a silicon carbide pellet at each step of the infiltration process. This is to show how the pores are being filled with the polymer precursor and to display the interaction the AHPCS is having with the silicon carbide pellets. As the number of infiltration steps is increased, it becomes more and more difficult to fill the open pores due to the previous infiltration and sintering steps. These open pores are essentially closed off after a given sintering and thus have the result of a lower density since they are open space. Therefore, an analysis of each phase of the infiltration is required to gain a better and more detailed knowledge on how these pores are being filled and what affects the AHPCS is having on the properties of the samples.

Each of these pellets was cut in half, again with a diamond saw, and their cross-sections were polished for analysis under the SEM as well as the optical microscope. Figure 28, Figure 30

and Figure 32 display the first, second, third infiltrated pellets, respectively under SEM observation. In addition, Figure 29, Figure 31 and Figure 33 display the first, second and third infiltrated pellets, respectively as obtained from the optical microscope. With these photos, it can be more easily seen how the AHPCS alters the microstructure of the silicon carbide pellets.

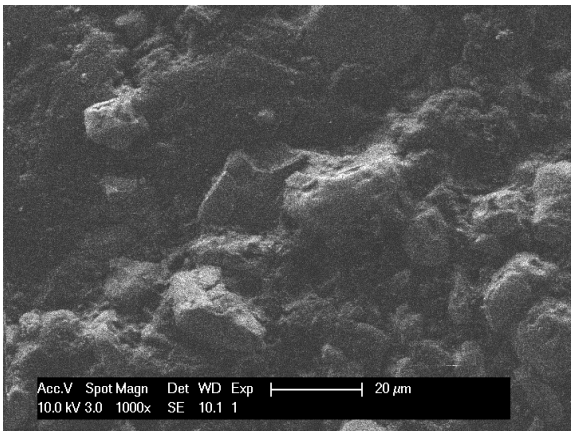

Figure 28 – One Time Infiltrated Silicon Carbide Pellet, SEM

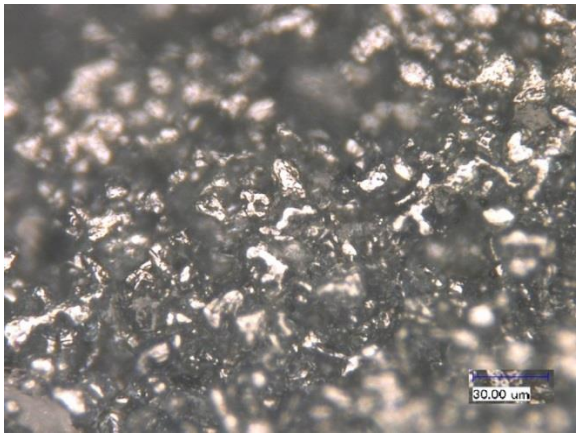

Figure 29 - One Time Infiltrated, Cross-Section Silicon Carbide, Optical Microscope

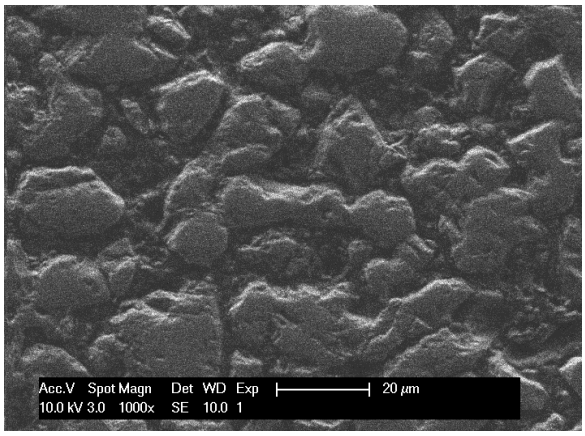

Figure 30 – Two Time Infiltrated Silicon Carbide Pellet, SEM

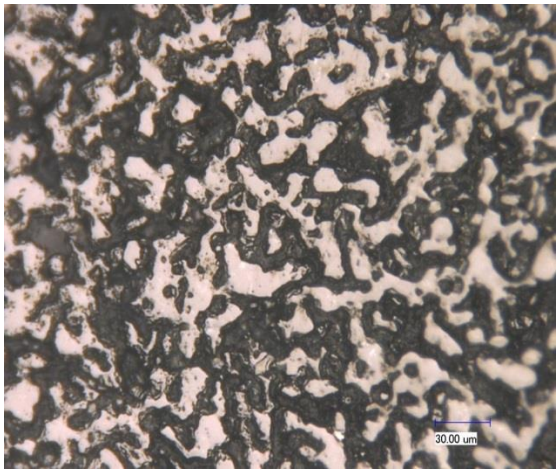

Figure 31 - Two Time Infiltrated, Cross-Section Silicon Carbide, Optical Microscope

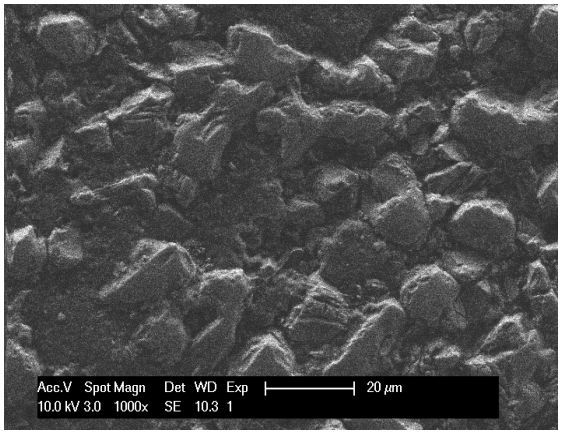

Figure 32 - Three-time infiltrated Silicon Carbide Pellet, SEM

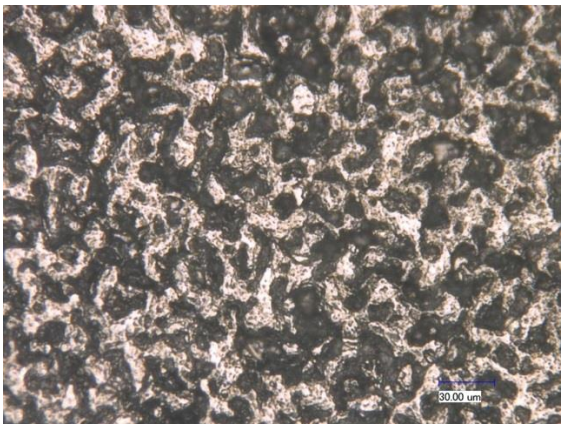

Figure 33 - Three Time Infiltrated, Cross-Section Silicon Carbide, Optical Microscope

Initial observations from analyzing each step of the infiltration process resulted in concern over whether grains were being pulled out. The initial thought was that the grains were being pulled out from the polishing technique, as the amount of time spent on the grinding phase of the polishing procedure was too long. However, after careful analysis it is believed that there is none to minimal grain pullout in any of these samples. As it can be seen from analyzing the images, the first infiltration has great amount of open pores. As the infiltration step progress, the number of visible pores begins to decrease. The starting silicon carbide particles are being altered, such that they are combining with their neighbors to form much larger sized particles. This is not uncommon in ceramics when undergoing sintering, as they can recombine with their neighbors and form large-looking particles. However, it is important to note that silicon carbide does not typically recombine with neighboring particles under such a low processing temperature. Usually this behavior is prevalent under much higher temperatures. This phenomenon is important to characterize due to the uniqueness of the recombination at the given temperature for silicon carbide. In addition to the necking that occurring between the silicon carbide particles, there also appears to be a layering affect, where the top layer appears crystalline while underneath there is potential that it is amorphous-like. Further techniques, such

as electron back scattering diffraction (EBSD), will need to be utilized to analyze the pellets to determine a more accurate representation of the phases present.

The next samples to be analyzed were the nickel nanoparticle pellets. Seen in Figure 34 is the 10 wt% four time infiltrated nickel silicon carbide pellet from a cross-sectional viewpoint. Where as in Figure 36, the four times infiltrated 5 weight percent nickel nanoparticle pellet cross section can be seen. From these photos, which were both taken under SEM, it can be seen that the microstructure is quite compact with isolated particles and no evidence of any necking of particles in either the 5 or 10 weight percent samples, as was the case in the AHPCS-only infiltrated silicon carbide pellets. In addition to the obtained SEM images, Figure 35 and Figure 37 display the optical microscope images obtained for the 10 weight percent and 5 weight percent nickel nanoparticle pellets, respectively. It is possible that the reaction created between the nickel and the silicon carbide is exothermic and further enhancing the sintering behavior of the sample. Through this addition of nickel nanoparticles it can be hypothesized that there is some liquid phase sintering occurring, as evidenced by the possibility as seen in the Ni-Si phase diagram. Through the liquid phase sintering, a higher density was achieved.

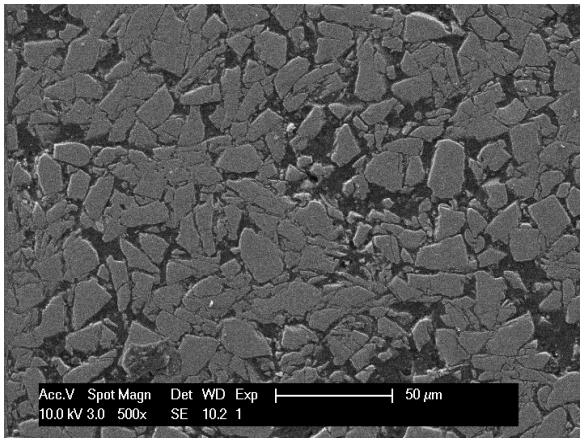

Figure 34 - 10 wt%, Four Time Infiltrated Nickel Nanoparticle Pellet, SEM

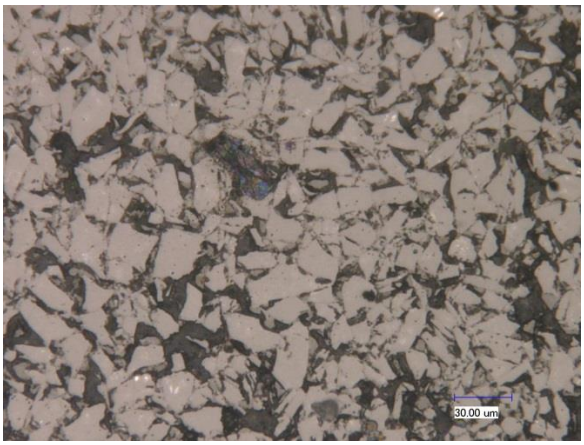

Figure 35 - 10 wt% Nickel, Cross-Section, Optical Microscope

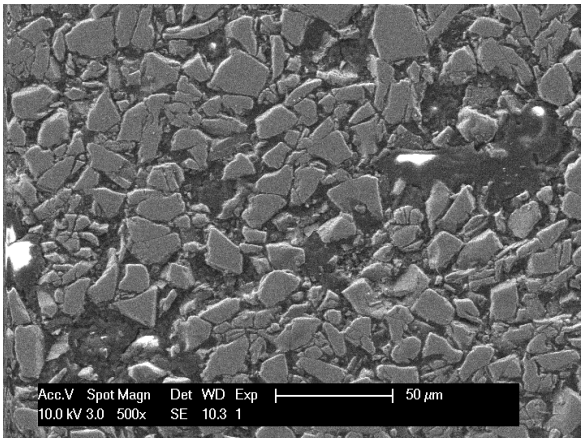

Figure 36 - 5 wt%, Four Time Infiltrated Nickel Nanoparticle Pellet

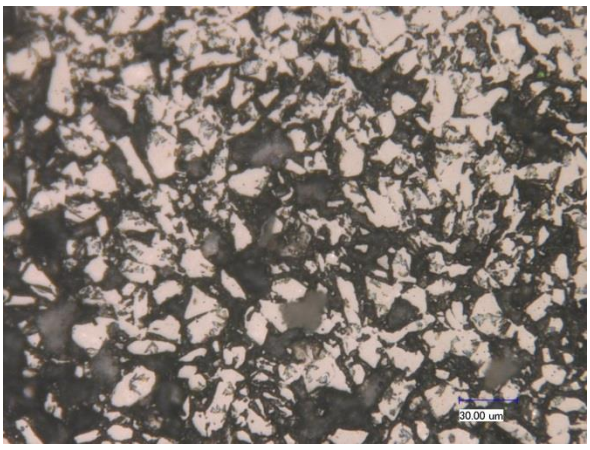

Figure 37 - 5 wt% Nickel Nanoparticle, Cross-Section, Optical Microscope

5.4 HARDNESS VALUES

Another parameter that was measured of the polished, four time infiltrated silicon carbide pellets as well as both the 5 and 10 weight percent nano-nickel infiltrated pellets, was the hardness value. The hardness value of standard silicon carbide is in the realm of 2800 [31] on the Vickers Hardness scale. For completeness, a hardness value for each infiltration step of the AHPCS-only infiltrated pellets was also obtained. It is important to properly characterize how the hardness changes as a function of the number of infiltrations. This allows for a greater understanding on how the polymer precursor is changing the microstructure to a more dense material. The unit of the values is HV, for Vickers hardness.

Table 10 displays the recorded averages for the hardness values of the four time infiltrated AHPCS-only, 5 and 10 weight percent silicon carbide pellets. As it can be seen from the table, the addition of nickel nanoparticles increased the hardness value. It is believed that this increase in hardness can be mostly attributed to the increase in density. In addition to the density, it is possible that the formation of nickel carbide and nickel silicide also played a role in the increase of hardness. Further investigations will need to be performed to confirm this. Although, this is not a substantial increase, it is one worth noting. As seen from the microstructure under the optical and scanning electron microscopes, a major difference was the agglomeration of particles in the AHPCS-only and the lack of agglomeration of particles in the nickel nanoparticle pellets. This difference can attribute to the variation seen in the hardness between samples. Numerous indents were made in various locations of the samples to obtain a more overall characteristic hardness of the sample.

Table 10 - Average Hardness Value for Each Pellet

Type of Pellet	Hardness Value (HV)	Standard Deviation	% Error in SiC [14]
AHPCS-only	2600	175	7.50
5 wt% Nickel	2700	106	4.30
10 wt% Nickel	2730	115	3.20

Seen in Figure 38, is an indent made on the surface of an AHPCS, sieved, polished silicon carbide pellet. This figure shows a sample calculation on how the other indents were characterized in order to determine the hardness of the sample. For completeness, Figure 39 displays a sample characterization from a 5% Ni-AHPCS silicon carbide pellet, where Figure 40 shows a sample characterization of a 10% Ni-AHPCS silicon carbide pellet. Typically seen in indents on the microstructure when analyzing the hardness values are cracks propagating from the corners of the indents, which is a signal of the resistance to plastic deformation in a given sample. Hardness testing of ceramics is quite challenging and with the large starting powder size it is possible that some indents were made between grains, which would alter the results of the hardness testing.

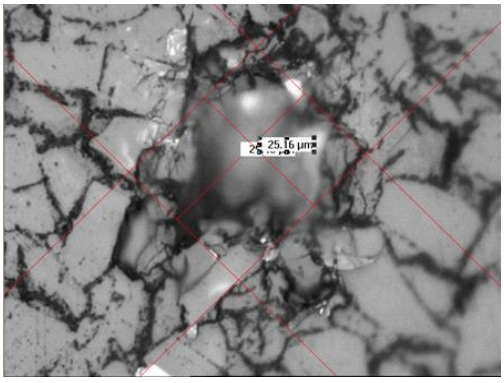

Figure 38 - Indent Characterization of AHPCS Silicon Carbide Pellet Hardness Value

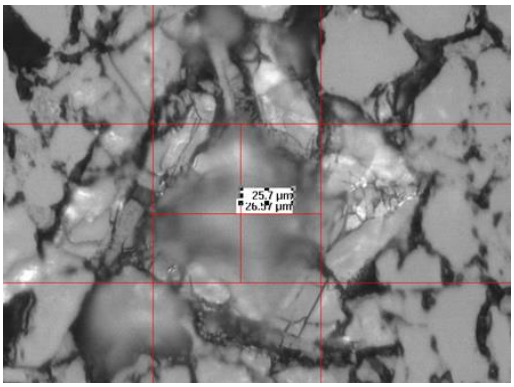

Figure 39 - Indent Characterization of 5% Ni-AHPCS Silicon Carbide Pellet Hardness Value

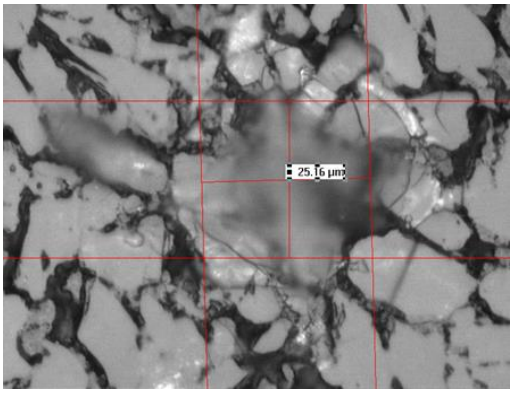

Figure 40 - Indent Characterization of 10% Ni-AHPCS Silicon Carbide Pellet Hardness Value

To better understand how the hardness value changes after each infiltration, the same calculations and analysis was performed to assess the performance of the AHPCS-only silicon carbide pellets. Table 11 displays the results for hardness value of each infiltration step, as well as the standard deviation. To ensure that the results are valid, multiple indents were made in varying locations. As it can be seen from this table the more infiltrations a pellet experiences, the higher the hardness value is obtained. This is because the number of open pores is reduced thus allowing for greater resistance when the indent is made onto the sample. With the first infiltration there are a substantial amount of open pores and thus has a low value of hardness.

Table 11 - Hardness Value for Each Infiltration Step of the AHPCS-only Pellets

Infiltration Step	Hardness Value	Standard Deviation
1st Infiltration	200	42
2nd Infiltration	800	40
3rd Infiltration	1700	142
4th Infiltration	2600	175

From obtaining the hardness value at each infiltration step, it could then be compared to the density at each infiltration. The following figure displays a semi-log plot of hardness versus density, for each infiltration step of the AHPCS-only pellets. As it can be seen from Figure 41, the correlation coefficient is very strong, at a value almost exactly one. This figure is strictly represented to show a correlation between two important parameters when analyzing the silicon carbide pellets. As the sample becomes more dense, the hardness value increases showing good correlation between the two parameters.

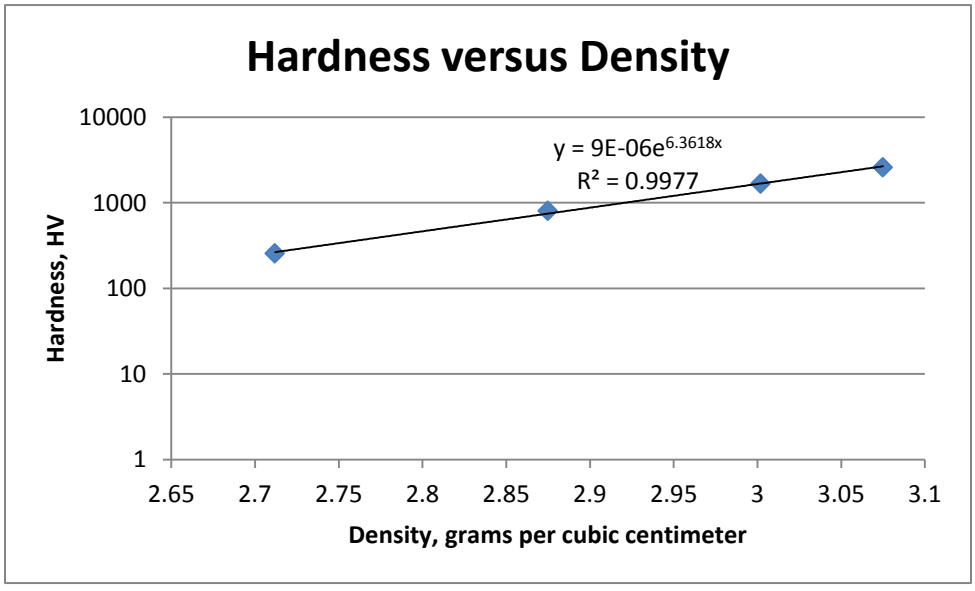

Figure 41 - Semi-Log Plot of Hardness vs. Density of Each Infiltration

5.5 ETCHING

Etching is a technique that is important to reveal important details of the microstructure of the sample in question. Through the etching of a material it is believed that the end result will show and allow for a better understanding of the grain boundaries in the sample. Grain boundaries are important to understand because most grain boundaries are typically the preferred sites of the inception of corrosion. They are also important to the mechanisms of creep in the material, which will play a role in the reactor.

To etch the silicon carbide pellets, a solution of 100 milliters of deionized water, 10 grams of potassium hydroxide and 10 grams potassium ferrocyanide was prepared. This solution is commonly referred to as Murakami's solution. Each of these chemicals was purchased from Sigma-Alrdich. From here, the polished silicon carbide pellet was submerged in the solution, at room temperature, for a minute, rinsed with deionized water and dried through the air. Once it was dry, it was examined under an optical microscope. This process was repeated several times, until noticeable results were achieved through visualization under the optical microscope. In Figure 42, the non-etched surface of the polished silicon carbide pellets at 5000 times the magnification. As wherein Figure 43 displays the etched silicon carbide pellet at 5000 times the magnification after 10 minutes submerged inside the prepared solution.

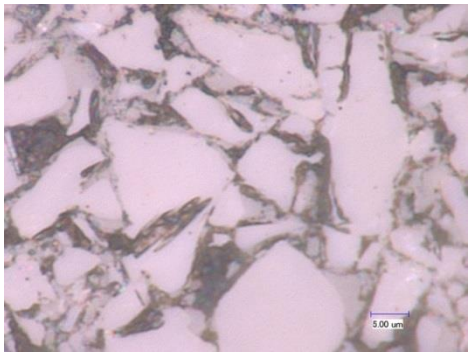

Figure 42 - Polished, Silicon Carbide Pellet, No Etching, 5000 Times Magnification

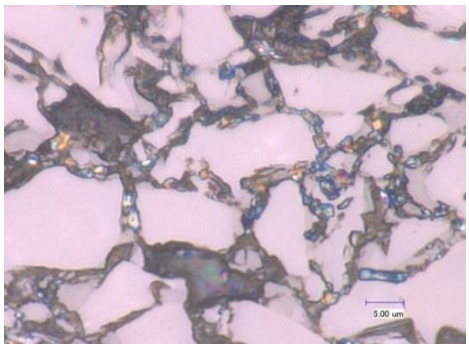

Figure 43 - Polished, Silicon Carbide Pellet, 10 Min Etching, 5000 Times Magnification

From the optical microscope, the pellets that were etched for 10 minutes were then analyzed under the scanning electron microscope. Figure 44 and Figure 45 display the images obtained from the SEM of the etched silicon carbide pellet. The final effect of etching using this technique was not as quantifiable as desired. In order to produce more desirable results from this etching process, many more experiments will need to be conducted. The desired outcome would be to comprehend the location of grain boundaries in the silicon carbide sample.

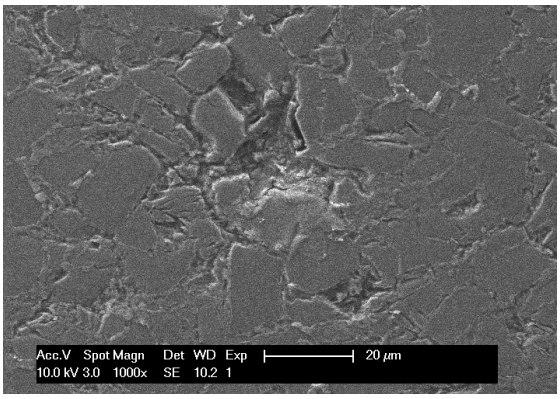

Figure 44 - SEM of 10 Minute Etched Silicon Carbide Pellet

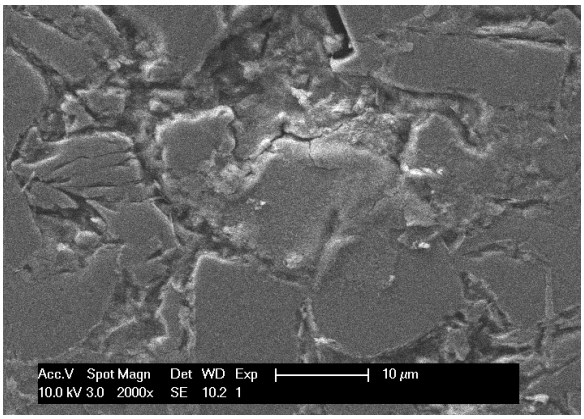

Figure 45 - SEM of 10 Minute Etched Silicon Carbide Pellet

5.6 FREEZE CASTING OF SILICON CARBIDE

The freeze casting method of silicon carbide produced samples that were not perfectly cylindrical as was the case with the pressed samples. Therefore, since these were not cylindrical or any definite shape in which a volume equation could be applied, an alternative method needed to be imposed. The alternative method that was applied was the Archimedes Method. This method involves obtaining the dry weight of the pellet on the Mettler Toledo weighing balance then placing the pellet under vacuum to completely expunge any air that may be present inside the pores. This vacuum process took over 24 hours to ensure that all the air and moisture was removed before submerging the pellet in water. The next measurement was to weigh the pellet suspended in water, followed by weighing the sample after removing any excess water from the surface of the pellet. The bulk density was equated by following Equation 8, whereas the apparent density was found through utilization of Equation 9.

$$\rho_{bulk} = (\text{Dry weight}) / (\text{Wet weight} - \text{Suspended weight})$$

Equation 8 - Bulk Density via Archimedes Method

$$\rho_{apparent} = (\text{Dry weight}) / (\text{Dry weight} - \text{Suspended weight})$$

Equation 9 - Apparent Density via Archimedes Method

Table 12 displays the results for each infiltration of the freeze casted silicon carbide sample. As it can be seen from this table, the density is lower, most directly due to the fact that is considerably a greater amount of open pores that were created via this process. Although, these samples were infiltrated with the AHPCS polymer precursor, it does not close nor fill the pores completely, thus resulting in a lower density. The bulk density calculation is representative of the solid, open and closed pores, whereas the apparent density is representative of the solid and closed pores only. Therefore, to find the percent of open pores a simple subtraction of the two densities is required. A major purpose of this processing technique is to create a porous silicon carbide ceramic with a rigid framework. Having the ability to construct a porous body with rigid framework can be applied to various applications other than fuel cladding.

Table 12 - Densities Obtained via Archimedes Method, Bulk and Apparent

	Bulk Density (g/cm^3)	% Silicon Carbide	Apparent Density (g/cm^3)	% Silicon Carbide
Annealed	1.477	46.01	2.864	89.24
1^{st} Infiltration	1.812	56.63	2.918	91.18
2^{nd} Infiltration	2.006	60.81	3.007	93.95
3^{rd} Infiltration	2.122	66.33	3.020	94.35

After the density of each infiltration was recorded, the freeze casted samples were then prepared to be analyzed under the scanning electron microscope. The pore channels are formed

through a templating technique where a non-ceramic is utilized as template for the pore structure. Ice crystals are the non-ceramic used in this study that are created and later removed through sublimation. First, the samples were cut perpendicular to the direction of the pore channel with a diamond saw. Then, the other samples of the same batch were cut parallel to the direction of the desired pore channels. Figure 46 and Figure 47 display the results obtained from analyzing the annealed freeze cast samples that were cut perpendicular to the pore channels. Figure 48 and Figure 49 show the first infiltration perpendicular to the pore channel, while Figure 50 and Figure 51 display the second infiltration. In the images of the first and second infiltrated freeze cast samples, there appears to be a substance on the silicon carbide particles. It is believed that this substance is the residual AHPCS that was left there as a result of the sintering process. In the perpendicular photos it is hard to accurately discern any direction of the pores from the freezing process. This characterization was utilized for completeness to verify any results and to gain a further understanding of the freezing direction.

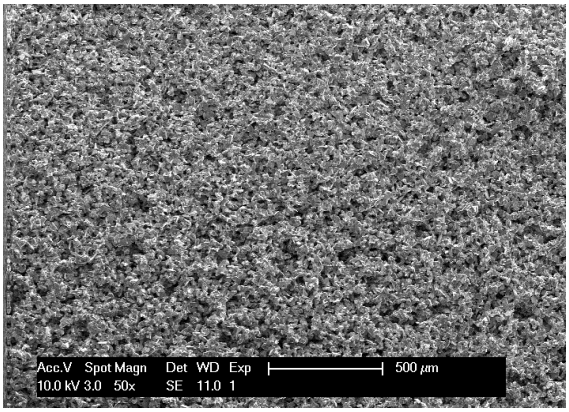

Figure 46 - Annealed, Freeze Cast Silicon Carbide, Perpendicular to Freezing Direction

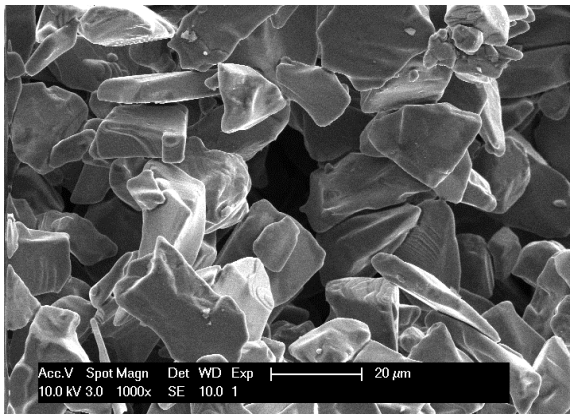

Figure 47 - Annealed, Freeze Cast Silicon Carbide, Perpendicular to Freezing Direction

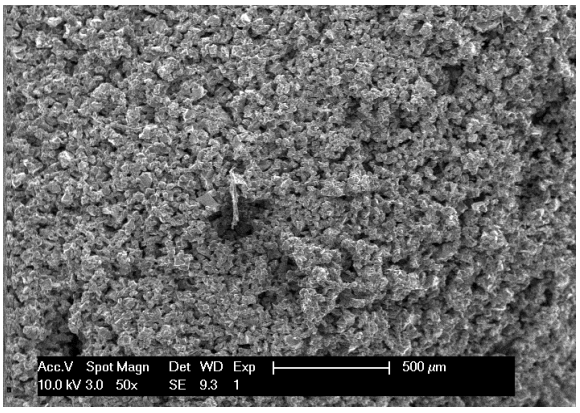

Figure 48 - 1st Infiltration of Freeze Cast Silicon Carbide, Perpendicular to Freezing Direction

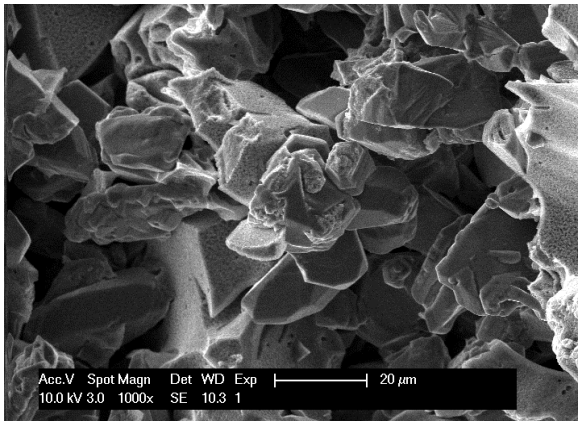

Figure 49 - 1st Infiltration of Freeze Cast Silicon Carbide, Perpendicular to Freezing Direction

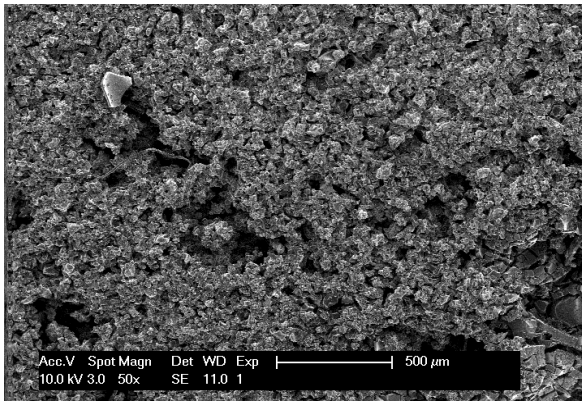

Figure 50 - 2nd Infiltration Freeze Cast Silicon Carbide, Perpendicular to Freezing Direction

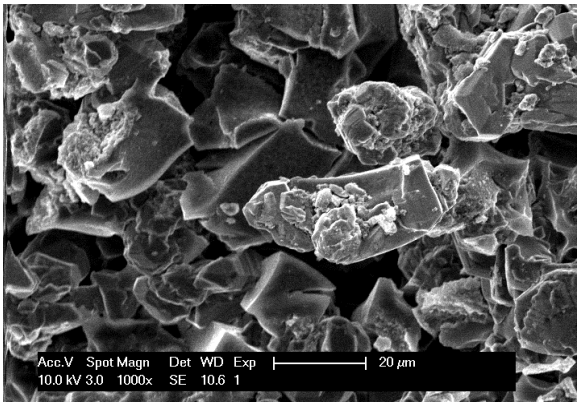

Figure 51 - 2nd Infiltration Freeze Cast Silicon Carbide, Perpendicular to Freezing Direction

Once the perpendicular SEM images were obtained, the samples were then cut parallel to the desired pore channel direction. By cutting the sample this way, it will allow for a much more clear analysis of the direction of the frozen pore channels. It is the goal to achieve pore channels with uni-directionality. Figure 52 and Figure 53 display the annealed freeze cast sample, while Figure 54 and Figure 55 illustrate the 1st infiltrated sample. Lastly, Figure 56 and Figure 57 exemplify the 2nd infiltrated freeze cast sample. Again, the substance that appears on the silicon carbide crystals is believed to be residual AHPCS from the sintering phase of this experimentation. From the following images, it is rather difficult to completely distinguish the direction of the pore channels. A likely reason for the inability to visually see these channels is caused by the large size of the starting silicon carbide particles. As previously outlined, the

starting particles for many of the successful freeze casting experiments have been in the single to sub-mircon sizes, whereas the starting silicon carbide particles used for this experiment were on the average of 37 microns. This large starting particle size doesn't allow for the pores to freeze in the desired direction due the interactions of the particles with each other, which lead to the chaotic and scattered freezing as depicted by the following images. It is believed that a smaller starting particle size will reduce the interactions between particles, thus allowing for a more clear direction of the pore channels.

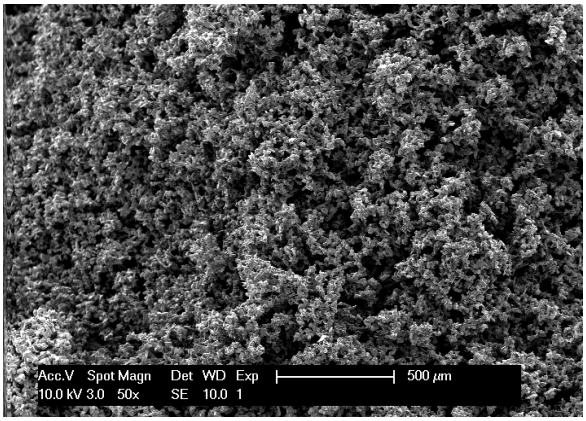

Figure 52 - Annealed, Freeze Cast Silicon Carbide, Parallel to Freezing Direction

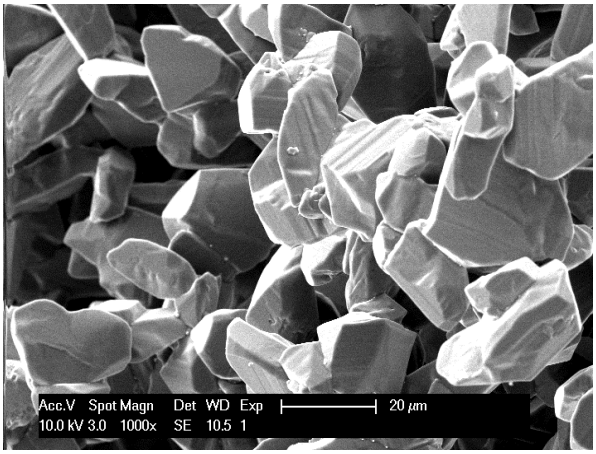

Figure 53 - Annealed, Freeze Cast Silicon Carbide, Parallel to Freezing Direction

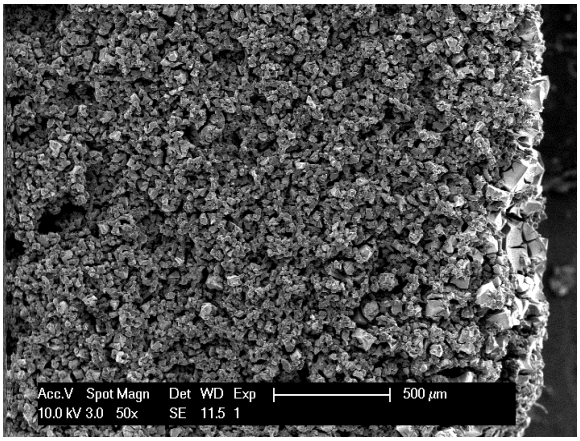

Figure 54 - 1st Infiltration of Freeze Cast Silicon Carbide, Parallel to Freezing Direction

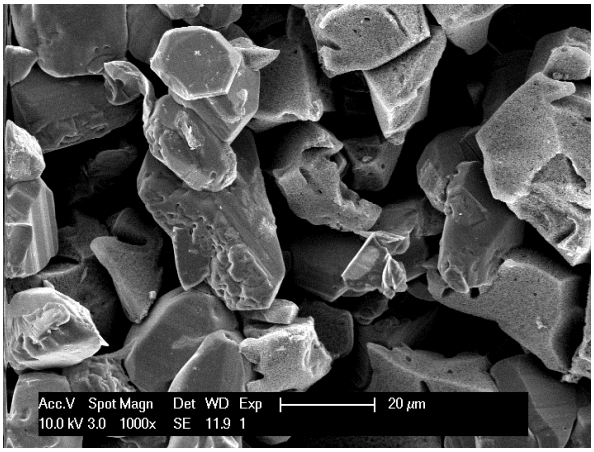

Figure 55 - 1st Infiltrated Freeze Cast Silicon Carbide, Parallel to Freezing Direction

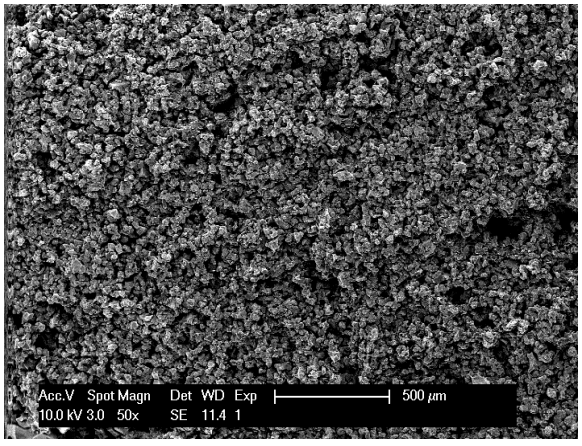

Figure 56 - 2nd Infiltrated Freeze Cast Silicon Carbide, Parallel to Freezing Direction

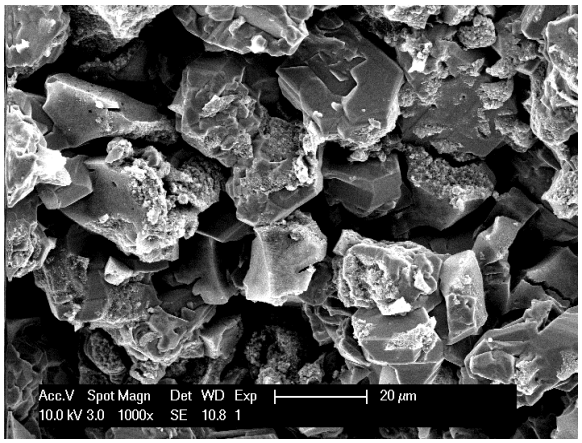

Figure 57 - 2nd Infiltrated Freeze Cast Silicon Carbide, Parallel to Freezing Direction

6.0 CONCLUSION AND FUTURE WORK

There is a definite increasing need for an advanced cladding material in operational nuclear reactors. In lieu of the recent incident at the nuclear facility in Fukushima, where water and steam reacted with the zirconium cladding, which lead to an increase in the hydrogen gas concentration. This increase directly led to the subsequent explosions which resulted in more structural damage as well as radiation release. With this incident and the idea to increase the safety margin even further, a new cladding material must be developed and implemented. Silicon carbide has been proposed as the leading material to replace the zirconium alloy and one benefactor is the fact that silicon carbide would not create the hydrogen gas that resulted in the catastrophic explosion seen in Fukushima. In addition to the chemical inertness silicon carbide would provide when reacting with high temperature water and steam, it is believed that it would also be able to handle higher fuel burnups than the zirconium alloy. The ability to handle higher fuel loads would likely result in longer periods between outages for a nuclear power plant facility. There are many positive attributes in regards to silicon carbide as a replacement for the current cladding material; however, it also possesses some challenges as well.

There have been several other manufacturing and processing techniques to produce silicon carbide. Up until now, these methods utilized high temperatures and pressures, the use of additives, highly toxic chemicals or a combination to enhance the sintering behavior of silicon carbide. Through this research it was discovered that a highly dense silicon carbide ceramic can

be produced without the use of high temperatures and pressures, additives or toxic gases. In this research highly dense, about 95 percent theoretical density of silicon carbide, ceramic was produced using a liquid polymer precursor through an infiltration and pyrolysis technique with a low processing temperature. In addition to the low processing temperature, fewer infiltration steps were required during this research in comparison to previous infiltration studies, whereas those experiments required upwards of six or more infiltrations. Therefore, this investigation produced a silicon carbide ceramic with more optimal parameters than previous studies.

In an attempt to further increase the sintering behavior of the silicon carbide, nickel nanoparticles were added to the liquid polymer precursor and infiltrated into the silicon carbide framework. Through this investigation it is believed that liquid phase sintering is a result of the addition of the nickel nanoparticles. This is first evidenced by the examining the phase diagram of nickel and silicon, where a liquid phase is present below the processing temperatures utilized in this experiment. In addition to examining the phase diagram, x-ray diffraction patterns were characterized and compared to standard diffraction patterns. Through comparison, it can be seen that the formation of nickel carbide as well as nickel silicide was witnessed. In previous investigations there was no mentioning of the formation of nickel carbide when nickel and silicon carbide interact. However, two major differences are that those studies did not make use of solid nanoparticles nor did they add the nickel to a liquid polymer precursor, where the silicon and carbon bonding is weaker. Therefore, with these two major differences, and knowing the binding energy of nickel carbide is greater than that of nickel silicide or silicon carbide, it is believed the formation of nickel carbide in this investigation is an accurate representation.

In regards to difference in density between the AHPCS-only and nickel nanoparticle, a slight increase was noticed through the addition of nickel nanoparticles. As for the Vickers

Hardness values obtained, it is believed that the increase in the nickel nanoparticle samples were attributed to the increase in density. When analyzing the scanning electron images, it can be ascertained that there was necking occurring between the particles in the AHPCS-only infiltrated sample. Whereas, in the nickel nanoparticle images there grains had a more defined shape, which was likely due to the enhanced liquid phase sintering behavior.

The last processing technique that was investigated was freeze casting. Through the methodology a porous silicon carbide ceramic with a rigid body was produced. Through a similar infiltration technique with a liquid polymer precursor, the density was increased while maintaining the solid framework of the body. However, the scanning electron images obtained through this process were poor and did not display the desired pore channel direction. It is believed that since the size of the starting particles were much greater than previous studies; this is the main reason the pore channels did not develop with uni-directionality. Further investigations will need to be pursued for this processing technique.

The investigation produced a highly dense silicon carbide material without the use of high temperatures and pressure, additives or toxic gases. Enhanced sintering was seen through the addition of nickel nanoparticles via liquid phase sintering. An addition processing technique, freeze casting, was investigated and produced a rigid framework with controlled porosity.

6.1.1 Future Work

6.1.1.1 Nuclear Investigation

In order to further verify the potential for silicon carbide to replace the current zirconium-based alloy as the cladding material for operation nuclear reactors, further tests must be conducted and replicated. A primary test should be focused on the irradiation of silicon carbide under different

levels of exposure. Since it is known that material properties change when exposed to irradiation, it is essential to fully comprehend how the manufactured silicon carbide will perform under given exposure levels of radiation. This testing will allow for a further understanding of the created silicon carbide at both the microstructure and macrostructure level.

In addition to the irradiation studies of silicon carbide, it is essential that the thermal conductivity be carefully examined and tested, under non-irradiated and irradiated conditions. As previously mentioned, the properties of irradiated materials can change greatly; therefore, it is crucial the thermal conductivity also be examined under both environments. By understanding and knowing the thermal conductivity will allow for a more developed calculation of the fuel centerline temperature during operation. The fuel centerline temperature is a key parameter in assessing the performance of the nuclear reactor, as too high or low of a temperature can lead to adverse effects in the entire system.

Lastly, the current cladding material is welded at the end joints to secure the uranium oxide fuel pellets inside; however, silicon carbide cannot be welded by traditional welding techniques. Therefore, an advanced technique in order to secure the ends of the silicon carbide cladding component must be developed. This testing is beyond the study of microstructure, but is an important development to fully utilize silicon carbide at the cladding component in an operating nuclear reactor.

6.1.1.2 Material Science Investigation

It is also important to characterize the microstructure development of both nickel nanoparticle cases. As seen with the AHPCS-only pellets, it was evidenced as an increase of necking in particles was apparent; therefore, it is necessary to develop the understanding on how the nickel nanoparticles affect the microstructure during each infiltration step. In addition to

advancing the knowledge on the development of the microstructure, it is crucial to utilize a transmission electron microscope to accurately determine the amorphous phase in the AHPS-only silicon carbide as well as determine the location of the nickel carbide and nickel silicide sites.

As for the freeze casting, in addition to testing a smaller starting particle size of silicon carbide, it would be interesting to infiltrate with the nickel nanoparticles to assess the performance and development of pore channels with the addition of these particles. Also, since this method leaves a large amount of pores in the sample, it would be beneficial to understand if this method would allow for application in other processes such as pore confined metal nanoparticle catalysts.

BIBLIOGRAPHY

[1] A. R. S. C. Z. R. P. Singh, "Bulk and Nanoscale Characterization of Silicon Carbide Derived from Preceramic Polymer Precursor," 2008.

[2] L. Hallstadius, S. Johnson, and E. Lahoda, "Cladding for high performance fuel," *Progress in Nuclear Energy,* vol. 57, pp. 71-76, 2012.

[3] K. Ahn, "Comparison of Silicon Carbide and Zircaloy4 Cladding during LBLOCA," 2006.

[4] C. P. Deck, H. E. Khalifa, B. Sammuli, T. Hilsabeck, and C. A. Back, "Fabrication of SiC–SiC composites for fuel cladding in advanced reactor designs," *Progress in Nuclear Energy,* vol. 57, pp. 38-45, 2012.

[5] D. C. A. S. Z. E. K. Chalabi, "Silicon Carbide: Properties and Applications," 2012.

[6] J. R. J. W. E. Windes; P. A. Lessing; Y. Katoh; L. L. Snead; E. Lara-Curzio; J. Klett; C. Henager, "Structural Ceramic Composites for Nuclear Applications," 2005.

[7] S. Bragg-Sitton, K. Barrett, I. van Rooyen, D. Hurley, and M. Khafizov, "Studying silicon carbide for nuclear fuel cladding," *Nuclear Engineering International,* vol. 58, pp. 37-40, May 2013.

[8] G. Griffith, "U.S Department of Energy Accident Resistant SiC Clad Nuclear Fuel Development," 2011.

[9] J. Wang, "Developing a High Thermal Conductivity Nuclear Fuel with SiC Additives," 2008.

[10] M. Rohde, "Reduction of the Thermal Conductivity of SiC by Radiation Damage," *Journal of Nuclear Materials,* p. 5, 1991.

[11] S. E. S. A. Agarwal, "Advances in Silicon Carbide Processing and Applications," 2004.

[12] H. A. E. S. B. H. Hmida, "Silicon Carbide: Synthesis and Properties."

[13] A. K. Singh, "Novel Fabrication of SiC Based Ceramics," 2009.

[14] L. L. Snead, T. Nozawa, Y. Katoh, T.-S. Byun, S. Kondo, and D. A. Petti, "Handbook of SiC properties for fuel performance modeling," *Journal of Nuclear Materials,* vol. 371, pp. 329-377, 2007.

[15] C. A. T. J. E. R. d. S. L. A. A. T. M. C. A. T. e. S. G. L. M. d. A. Damy, "Comparison of the Mechanical Properties and Corrosion Resistance of Zirlo and Other Zirconium Alloys," 2007.

[16] I. A. E. Agency, "Thermophysical properties database of materials for light water reactors and heavy water reactors," 2006.

[17] R. A. F. G. C. Patterson, "In-Reactor Creep of Zirconium Alloys," 2009.

[18] C. A. L. M. S. T. S. T. H. M. A. Y. K. A. Kohyama, "Joining of SiC Composites for Fusion Energy Applications," *Journal of Nuclear Materials,* p. 3, 2000.

[19] E. Herderick, "A Novel Approach to Joining Silicon Carbide."

[20] H. Feinroth, "Silicon Carbide Triplex Nuclear Fuel Cladding An Alternative to Zircaloy That Avoids Severe Core Damage During Accidents," 2012.

[21] A. W. Weimer, "Carbide, Nitride, Boride Materials Synthesis and Processing," 1997.

[22] S. C. Zunjarrao, "Polymer Derived Ceramics: Processing Structure Property Relationships," 2001.

[23] J. L. Robichaud, M. Aghajanian, C. Emmons, S. Rummel, P. Barber, C. Robb, *et al.*, "Effect of grain size on microstructure, properties, and surface roughness of reaction bonded SiC ceramics," vol. 8837, p. 88370J, 2013.

[24] G. B. Guiseppe Magnani, Gian L Minoccari, Luigi Pilotti, "Pressureless Sintering and Properties of alpha-SiC-B4C Composite," *Journal of the European Ceramic Society,* 2001.

[25] M. M. Young-Wook Kim, Hideyuki Emoto, June-Gunn Lee, "Effect of Initial alpha-Phase Content on Microstructure and Mechanical Properties of Sintered SiC," *Journal of American Ceramic Soceity,* 1998.

[26] A. B. D. Sciti, "Effects of additives on densification, microstructure and properties of liquid-phase sintered silicon carbide," *Journal of Material Science,* 2000.

[27] L. K. L. Falk, "Microstructural development during liquid phase sintering of silicon carbide ceramics," *Journal of the European Ceramic Society,* 1996.

[28] A. Can, M. Herrmann, D. S. McLachlan, I. Sigalas, and J. Adler, "Densification of liquid phase sintered silicon carbide," *Journal of the European Ceramic Society,* vol. 26, pp. 1707-1713, 2006.

[29] C. Shih, J. S. Tulenko, and R. H. Baney, "Low-temperature synthesis of silicon carbide inert matrix fuel through a polymer precursor route," *Journal of Nuclear Materials,* vol. 409, pp. 199-206, 2011.

[30] O. Borrero-López, A. L. Ortiz, F. Guiberteau, and N. P. Padture, "Effect of liquid-phase content on the contact-mechanical properties of liquid-phase-sintered α-SiC," *Journal of the European Ceramic Society,* vol. 27, pp. 2521-2527, 2007.

[31] K. A. M. L. V. Interrante, "Processing, Fracture Toughness, and Vickers Hardness of Allylhydridopolycarbosilane-Derived Silicon Carbide," *Journal of American Ceramic Soceity,* p. 4, 2003.

[32] M. B. M. Calabrese, "Effect of 1600 C Heat Treatment on C/SiC Composites Fabricated by Polymer Infiltration and Pyrolysis with AHPCS," *Journal of American Ceramic Soceity,* p. 3, 2002.

[33] C. Shih, J. S. Tulenko, and R. H. Baney, "The effect of mixing methods and polymer infiltration and pyrolysis (PIP) cycles on the densification of silicon carbide inert matrix fuel through a polymer precursor route," *Journal of Nuclear Materials,* vol. 419, pp. 63-71, 2011.

[34] C. M. Pekor, "The Effect of Water-Soluable Polymers on the Microstructure and Properties of Freeze-Cast Alumina Ceramics," 2010.

[35] T. F. Z.-Y. D. M. A. T. O. Y. Goto, "Pore structure of porous ceramics synthesized from water-based slurry by freeze-dry process," *Journal of Material Science,* p. 4, 2001.

[36] J. M. F. F. H. M. M. Diz, "Effect of Solids Loading on Slip-Casting Performance of Silicon Carbide Slurries," *Journal of American Ceramic Soceity,* p. 7, 1999.

[37] A. K. Singh, S. C. Zunjarrao, and R. P. Singh, "Processing of uranium oxide and silicon carbide based fuel using polymer infiltration and pyrolysis," *Journal of Nuclear Materials,* vol. 378, pp. 238-243, 2008.

[38] F. I. Hurwitz, "Suspension of Silicon Carbide Powders in AHPCS: Control of Rheology."

[39] P. Greil, "Near Net Shape Manufacturing of Polymer Derived Ceramics," *Journal of the European Ceramic Society,* p. 9, 1998.

[40] A. N. P. Nash, "The Ni-Si System," 1987.

[41] R. S.-F. K. Bhanumurthy, "Interface Reactions Between Silicon Carbide and Metals," 2001.

[42] K. L. J.S. Park, J.H. Perepezko, "Kinetics control of silicon carbide/metal reactions," *Material Science and Engineering*, 1999.